DAVID W. TAYLOR NAVAL SHIP
RESEARCH AND DEVELOPMENT CENTER

Bethesda, Maryland 20084

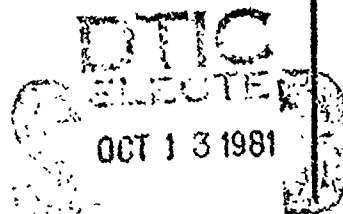## FLOW CHARACTERISTICS OF A TRANSOM STERN SHIP

by

John O'Dea
Douglas Jenkins
Toby Nagle

APPROVED FOR PUBLIC RELEASE: DISTRIBUTION UNLIMITED

DTIC
ELECTE
OCT 1 3 1981

SHIP PERFORMANCE DEPARTMENT
RESEARCH AND DEVELOPMENT REPORT

September 1981

MAJOR DTNSRDC ORGANIZATIONAL COMPONENTS

```
                        ┌─────────────────────────┐
                        │        DTNSRDC          │
                        │    COMMANDER      00    │
                        │  TECHNICAL DIRECTOR     │
                        │                   01    │
                        └─────────────────────────┘
                                   │
        ┌────────────────────────┐   ┌────────────────────────┐
        │   OFFICER-IN-CHARGE    │───│   OFFICER-IN-CHARGE    │
        │   CARDEROCK      05    │   │   ANNAPOLIS      04    │
        └────────────────────────┘   └────────────────────────┘

        ┌────────────────────────┐
        │       SYSTEMS          │
        │    DEVELOPMENT         │
        │    DEPARTMENT     11   │
        └────────────────────────┘

        ┌────────────────────────┐   ┌────────────────────────┐
        │  SHIP PERFORMANCE      │   │    AVIATION AND        │
        │   DEPARTMENT      15   │───│   SURFACE EFFECTS      │
        │                        │   │   DEPARTMENT     16    │
        └────────────────────────┘   └────────────────────────┘

        ┌────────────────────────┐   ┌────────────────────────┐
        │     STRUCTURES         │   │    COMPUTATION         │
        │   DEPARTMENT     17    │───│  AND MATHEMATICS       │
        │                        │   │   DEPARTMENT     18    │
        └────────────────────────┘   └────────────────────────┘

        ┌────────────────────────┐   ┌────────────────────────┐
        │   SHIP ACOUSTICS       │   │   PROPULSION AND       │
        │    DEPARTMENT     19   │───│  AUXILIARY SYSTEMS     │
        │                        │   │   DEPARTMENT     27    │
        └────────────────────────┘   └────────────────────────┘

        ┌────────────────────────┐   ┌────────────────────────┐
        │     MATERIALS          │   │      CENTRAL           │
        │   DEPARTMENT     28    │───│  INSTRUMENTATION       │
        │                        │   │   DEPARTMENT     29    │
        └────────────────────────┘   └────────────────────────┘
```
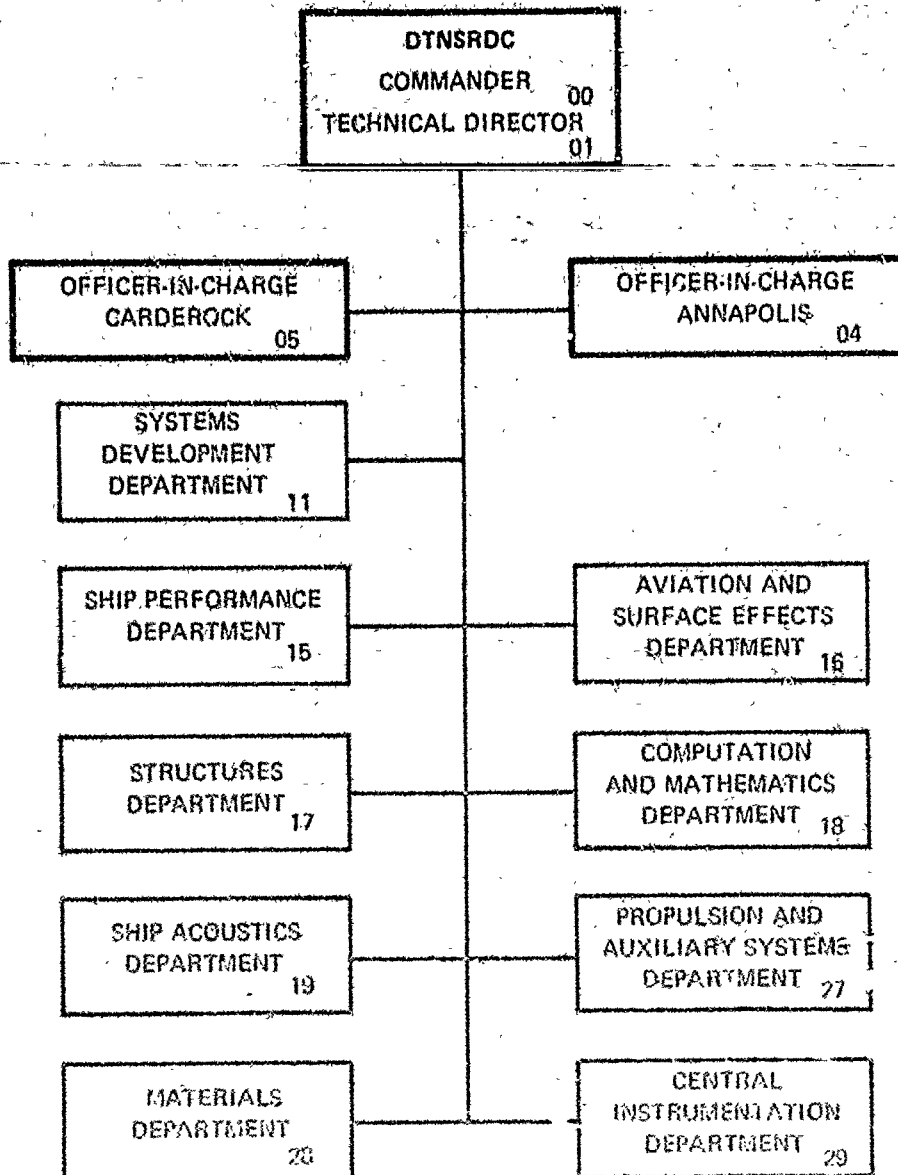
REPORT DOCUMENTATION PAGE		READ INSTRUCTIONS BEFORE COMPLETING FORM
1. REPORT NUMBER DTNSRDC-81/057	2. GOVT ACCESSION NO. AD-A106 264	3. RECIPIENT'S CATALOG NUMBER
4. TITLE (and Subtitle) FLOW CHARACTERISTICS OF A TRANSOM STERN SHIP		5. TYPE OF REPORT & PERIOD COVERED Final 6. PERFORMING ORG. REPORT NUMBER
7. AUTHOR(s) John O'Dea Douglas Jenkins Toby Nagle		8. CONTRACT OR GRANT NUMBER(s)
9. PERFORMING ORGANIZATION NAME AND ADDRESS David W. Taylor Naval Ship Research and Development Center Bethesda, Maryland 20084		10. PROGRAM ELEMENT. PROJECT, TASK AREA & WORK UNIT NUMBERS (See reverse side)
11. CONTROLLING OFFICE NAME AND ADDRESS Naval Sea Systems Command (03R) Washington, D.C. 20362		12. REPORT DATE September 1981 13. NUMBER OF PAGES 53
14. MONITORING AGENCY NAME & ADDRESS(If different from Controlling Office) Naval Sea Systems Command (03R2) Washington, D.C. 20362		15. SECURITY CLASS. (of this report) UNCLASSIFIED 15a. DECLASSIFICATION/DOWNGRADING SCHEDULE

16. DISTRIBUTION STATEMENT (of this Report)

APPROVED FOR PUBLIC RELEASE: DISTRIBUTION UNLIMITED

17. DISTRIBUTION STATEMENT (of the abstract entered in Block 20, if different from Report)

18. SUPPLEMENTARY NOTES

19. KEY WORDS (Continue on reverse side if necessary and identify by block number)

Transom Sterns
Ship Resistance
Wave Resistance

20. ABSTRACT (Continue on reverse side if necessary and identify by block number)

A series of experiments was conducted on a model of a typical transom stern destroyer hull in order to obtain a detailed set of measurements of flow characteristics around such a hull. Measurements included total drag, wave drag, sinkage and trim, pressure, and wave elevation both alongside the hull and behind the transom. Predictions of these characteristics were made using two free surface potential flow computer programs, and were compared to

(Continued on reverse side)

DD FORM 1473 EDITION OF 1 NOV 65 IS OBSOLETE
1 JAN 73
S/N 0102-LF-014-6601

(Block 10)

    Program Element 61153N
    Project Number SR 02301
    Task Area SR 023 0101
    Work Unit 1524-705

(Block 20 continued)

the measurements. The correlation between predictions and experimental measurements was generally satisfactory, indicating that such computer programs may be useful tools in future investigations of the properties of transom stern flow.

Accession For

NTIS GRA&I

DTIC TAB

Unannounced

Justification

By

Distribution/

Availability Codes

Avail and/or

Dist | Special

A

TABLE OF CONTENTS

LIST OF FIGURES

---

v

NOTATION

		Dimensions
A_{BL}	Area of ram bow in longitudinal plane	L^2
A_T	Section area of transom below DWL	L^2
A_X	Maximum section area	L^2
B	Maximum beam of ship	L^2
B_T	Beam of ship at transom	L
C_F	Frictional resistance coefficient $= R_F/(1/2\rho SV^2)$	–
C_P	Dynamic pressure coefficient $= -2gh/V^2$	–
C_R	Residuary resistance coefficient $= R_R/(1/2\rho SV^2)$	–
C_T	Total resistance coefficient $= R_T/(1/2\rho SV^2)$	–
C_W	Wavemaking resistance coefficient $= R_W/(1/2\rho SV^2)$	–
C_X	Maximum transverse section area coefficient $= A_X/BT$	–
F_n	Froude number $= V/(gL)^{1/2}$	–
FB/L	Longitudinal center of buoyancy from FP divided by length of ship	–
f_{BL}	Area coefficient of ram bow $= A_{BL}/LT$	–

		Dimensions
f_T	Sectional area coefficient for a transom stern $= A_T/A_X$	–
g	Acceleration due to gravity	L/T^2
h	Depth	L
i_B	Buttock slope at $1/4$ B_T at station $L/20$ from the aft end of the DWL (measured in degrees)	–
i_E	Half angle of entrance (measured in degrees)	–
i_R	Half angle of run (measured in degrees)	–
L	Length of ship	L
R_F	Frictional resistance	LM/T^2
R_R	Residuary resistance $= R_T - R_F$	LM/T^2
R_T	Total resistance	LM/T^2
R_W	Wavemaking resistance	LM/T^2
S	Wetted surface	L^2
$\textcircled{S}$	Froude's wetted surface coefficient $= S/\nabla^{2/3}$	–
T	Draft	L
T_A	Draft at AP	L

		Dimensions
V	Ship speed	L/T
y	Distance out from centerline of model	L
z	Bow and stern trim	L
$\Delta/(0.01L)^3$	Displacement-length ratio (tons/ft^3)	M/L^3
η	Wave elevation above calm water free surface	L
∇	Displacement volume	L^3
ϕ	Longitudinal prismatic coefficient $= \nabla/A_X L$	-
ρ	Density of water	M/L^3

LIST OF ABBREVIATIONS

AP	Aft perpendicular
DTNSRDC	David W. Taylor Naval Ship Research and Development Center
DWL	Designed waterline
FP	Forward perpendicular

ABSTRACT

A series of experiments was conducted on a model of a typical transom stern destroyer hull in order to obtain a detailed set of measurements of flow characteristics around such a hull. Measurements included total drag, wave drag, sinkage and trim, pressure, and wave elevation both alongside the hull and behind the transom. Predictions of these characteristics were made using two free surface potential flow computer programs, and were compared to the measurements. The correlation between predictions and experimental measurements was generally satisfactory, indicating that such computer programs may be useful tools in future investigations of the properties of transom stern flow.

ADMINISTRATIVE INFORMATION

INTRODUCTION

Transom sterns have been used for many years on displacement vessels with relatively high design speeds. It has been found empirically that an immersed transom generally had higher resistance than an equivalent conventional cruiser stern at low speeds, while this trend reversed as speed increased, so that a transom stern hull showed favorable resistance characteristics at high speeds (typically for Froude numbers (F_n) greater than approximately 0.3). A qualitative explanation for this behavior is that, at low speeds, the sharp corner of the transom provides a point of flow separation resulting in low pressure on the transom and a drag penalty. At high speeds, the flow breaks cleanly from the transom corner and the depression in the free surface behind the transom acts as a fictitious extended afterbody. This fictitious afterbody increases the effective hull length for generating wave drag and thus reduces the effective Froude number, but without any frictional drag penalty for this extended length.

Thus, a transom stern represents a trade-off in resistance at low and high speeds. The choice of afterbody shape is further complicated by other hydrodynamic

1

considerations besides resistance, such as propulsive efficiency, vibrations, and seakeeping. It must also be recognized that, as a practical matter, hull design decisions will also be driven by non-hydrodynamic considerations. In the case of stern shape, a transom stern will generally result in increased waterline and deck areas, and internal volume, when compared to a cruiser stern. All of these parameters may have a significant impact on the overall ship design.

It order to make trade-offs in a ship design, it is important for the designer to be able to estimate the calm water resistance. For transom sterns in particular, the effect of various stern shape parameters on resistance should be understood, in order that parametric changes in hull design can include reasonable estimates of the resulting changes in resistance. Unfortunately, the guidance available for estimating the resistance of a transom stern hull is quite limited. Much of the published information on this type of hull is in the form of systematic series model test results. Results of the most extensive series investigations are given by Marwood and Silverleaf,[1]* Yeh,[2] Lindgren and Williams,[3] and Bailey.[4] These series generally are concerned with hull forms designed for very high speed operation (F_n greater than 1.0 typically), such as patrol craft. Furthermore, because of practical limits on the number of hulls which can be built and tested in a series, these series results include systematic variation of only a few overall hull geometric parameters such as block coefficient, displacement-length ratio, and length-beam ratio. Transom geometry details were generally fixed in each series by the selection of a parent hull form, and the transoms of these series were generally quite large because of the very high design speeds. As a result, a large penalty in resistance would be suffered by these hulls at low speed, compared to a conventional hull form, and they are not suitable for ships designed to run at intermediate speeds such as destroyers or cruisers.

Large displacement ships such as destroyers or cruisers often have an operational envelope which requires them to operate efficiently at both a maximum speed based on installed power and a cruising speed which is significantly lower. These speeds may lie on either side of the transition region where a transom stern changes from favorable to unfavorable when compared to a more conventional stern. That is, the resistance of a transom stern hull may be somewhat higher than that of a

---

*A complete listing of references is given on page 41.

conventional hull at cruising speed, while the opposite may be true at maximum design speed. Therefore, accurate information on the resistance of transom stern hulls in an intermediate speed range (typically $0.25 < F_n < 0.50$) is necessary in order to determine if a transom stern is desirable for a particular design and, if so, what the details of the transom geometry should be to minimize resistance.

Published experimental information for transom stern hulls in this intermediate speed range is even more limited than for the very high speed range. St. Denis[5] has presented some general design guidelines for transom sterns, based on a series of destroyer model tests. Saunders[6] also provides some general design guidance, apparently based on empirical results. A systematic series of ten high speed merchant hulls with transom sterns is reported by Van Mater et al.,[7] but again transom geometry was held fixed throughout the series. Experimental data on transom stern hulls have also been published by Breslin and Eng[8] and Michelsen et al.,[9] but these were concerned with only two or three hull forms, and provide little direct information on the effect of transom shape on resistance.

Analytical work directed specifically at transom stern hull drag is also quite limited, and has been concerned only with the wavemaking (potential flow) component of resistance. Yim[10,11] has represented a transom stern as a transverse line singularity and combined this with a slender body wave drag theory to estimate some low-drag hull forms. Baba and Miyazawa[12] have represented the transom by a rectangular pressure distribution at the stern. Their results indicated that a tunnel-shaped afterbody and transom would have low drag, which was confirmed experimentally. Recently Vanden-Broeck[13] and Haussling[14] have studied the two-dimensional potential flow behind transom sterns, satisfying the exact free-surface boundary conditions.

Several three-dimensional potential flow computer programs have been developed over the last several years by Chang and Pien[15] and Dawson.[16] These programs solve for the three-dimensional potential flow about a hull, without any geometrical assumption of slenderness, using source-distribution and panel techniques. Recently in the workshop on Ship Wave Resistance Computations, both Dawson[17] and Chang[18] made computations with their programs for the R/V ATHENA, a high-speed transom stern hull. These calculations showed encouraging comparison to model test results. In addition,

3

two important points were brought out in this workshop. Dawson stressed the importance of sinkage and trim calculations, and their effect on wave drag of a hull which is free to trim. Chang furthermore pointed out that a considerable amount of the residuary drag coefficient was due simply to the hydrostatic term in Bernoulli's equation, which was nonzero when the transom was dry. This hydrostatic imbalance increases at high speed when a hull is free to trim down at the stern, and Chang hypothesized that this change in hydrostatic drag was the main cause of increased residual drag when a hull was allowed to trim.

The availability of these three-dimensional panel methods, including their apparent applicability to transom stern hulls, suggested that a combined analytical and experimental approach be pursued toward understanding the hydrodynamics of transom sterns. Because systematic model tests are very expensive, a logical alternative would be to perform a wide range of systematic parametric variations numerically, using these computer programs, rather than building and testing physical models in the towing tank. However, before this could be attempted with confidence, further correlation between the predictions from these programs and model test results was needed. The purpose of this report is to provide one such correlation for a single, typical transom stern hull. The experiments were designed to obtain detailed measurements, not just of drag, but of various other details of the flow both on the hull and in its vicinity. The detailed comparison between theory and measurement will provide an indication of the applicability of these programs, and of their limitations and areas for improvement.

ANALYTICAL PREDICTION METHODS

The computational methods used for predicting flow around a transom stern hull will be briefly described here. More detailed descriptions are provided by Dawson[16,17] and Chang.[15,18] Both programs have several points in common. Both consider the potential flow component only, and both solve for the potential by employing Green's theorem. This allows one to express the potential in terms of surface integrals of singularities on the fluid boundaries, which leads to an integral equation which must be solved for the singularity densities. Once the densities are known, the complete solution including potential, velocities, and

pressures is easily found. Integration of the pressures results in an axial force
(the drag) plus a vertical force and pitch moment which cause a floating hull to
change its trim. Other forces and moments are zero due to symmetry of the hull. The
actual calculations are carried out by discretizing the integral equation by dividing
boundary surfaces into discrete, flat quadrilateral panels and by assuming that the
unknown source density is constant on each panel. The integral equation is thus
replaced by a series of simultaneous algebraic equations, which can be put in matrix
form. The solution is then obtained by reduction or inversion of the matrix
equations.

Although both Chang's and Dawson's programs have these similarities, there is
one fundamental difference between them. The fundamental singularity used in Chang's
program is the Kelvin source. This has the fundamental singular behavior of a three-
dimensional point source, and in addition contains terms such that the source
satisfies the free surface boundary condition, the radiation condition at infinity,
and the zero-normal-velocity condition on the bottom of the fluid domain. As a
result, the boundary integration required by Green's Theorem must be carried out
only on the surface of the hull. Dawson's program (XYZFS) approaches the problem
in a somewhat different way. First the hull shape is combined with its image
(reflected about the free surface) to form a double body, and the potential flow for
this case solved in an infinite fluid with no free surface. The free surface condi-
tion, linearized in terms of the double body solution, is then introduced on the
undisturbed free surface (the plane of symmetry of the double body). In order to
satisfy this condition, additional panels must be introduced on the undisturbed free
surface, and a new set of source densities solved which satisfy the hull surface and
free surface boundary conditions simultaneously.

Another difference between the two computer programs is that the XYZFS iter-
atively redefines the panels describing the hull shape, based on the calculations of
sinkage and trim. Thus, if the bow rises and the stern sinks at high speed, some
panels near the bow may be deleted, while additional panels near the waterline at
the stern may be added.

Other differences between the two programs may be considered as by-products of
the particular techniques or choice of output details and format, rather than

fundamental differences in the theory. For instance, since panels are distributed on the free surface near the hull in the XYZFS program, wave elevations are calculated almost automatically. These are not included in the output of Chang's program although presumably it would be a straightforward matter to include this.

One final and perhaps significant difference between the two programs is also a result of the different techniques. The XYZFS program involves solving a relatively larger number (because of the free surface panels) of algebraic equations in which the coefficients are relatively simple to compute because only simple Rankine sources are used. On the other hand, Chang's program requires solving a relatively smaller number of equations (panels only on the hull surface) but each coefficient is considerably more time comsuming to compute, because of the free surface terms in the Havelock source. To some extent. these effects cancel so that the computing costs of the two programs are roughly similar. However, the memory storage requirements can be grossly different. For example, the surface of the hull used as a test case in this report was divided into approximately two hundred panels for both programs (although the panels were not exactly the same in both programs), but the free surface was divided into approximately three hundred more panels in the XYZFS program. Thus, the matrix of coefficients in Chang's program would require storage for approximately $(200)^2 = 40,000$ coefficients, while the matrix in the XYZFS program would require storage for approximately $(200+300)^2 = 250,000$ coefficients. This large a number can tax the available memory of even the largest computer available today. If an unusual hull form, such as one with a large bulbous bow, were to be paneled, computer memory size may become a limiting factor for the XYZFS program.

The spatial resolution of the hull and free surface, as defined by the number and size of panels, also has an effect on the range of Froude numbers for which it is feasible to calculate wave drag. The lower limit of speed is affected by the requirement to have small enough panels to resolve the wavelength of the free wave generated by the hull. In the present case, no wave drag predictions were made below a Froude number of 0.31. Conversely, the highest speed to be calculated may, in the case of the XYZFS program, require large numbers or sizes of panels defining the free surface. The final set of five Froude numbers at which calculations (and experimental measurements) were made was $F_n = 0.31, 0.34, 0.40, 0.45, 0.50$. This choice was based on prior knowledge of the shape of the residuary resistance curve for this hull and of general operating speed range for this type hull.

EXPERIMENTAL MEASUREMENTS

The hull model chosen for the experiments (Model 5322) has proportions which are typical of those of a modern naval surface combatant ship. An abbreviated lines plan is shown in Figure 1, and the principal characteristics of the hull form are presented in Table 1. The model length between perpendiculars is 5.99 m. A trip wire of 0.024-in. diameter (0.6 mm) was installed parallel to the stem line at station 1, and 1/8-in. (3 mm) outside diameter tubes were flush mounted at various locations on the afterbody to measure pressures on the bottom. The model was instrumented to measure total drag both mechanically, using a standard floating girder and pan weight balance, and electronically, using a modular force block. Electronic trim gages were installed to measure change of level (trim) at stations 0 and 20. All experiments were performed with a bare hull (no appendages).

The pressure taps in the hull were connected through flexible tubing to a multiple valve and manifold system mounted on the towing carriage. This system permitted each pressure line to be sequentially purged with air and measured by a single electronic pressure transducer, eliminating problems associated with calibrating many different transducers. A detailed description of this system is provided by Troesch et al.[19]

Wave profiles on the side of the hull were recorded by marking the elevation at each station, and wave elevations behind the transom were recorded both photographically and by measuring with a contact gage at several stations behind the transom. The wave elevation along a longitudinal cut at a point equal to two and one-half model beams off centerline was also recorded, using a resistance-wire type wave probe attached to a boom mounted to the side of the basin. This longitudinal wave cut was used to obtain an estimate of the wavemaking component of the drag, using the analysis method described by Sharma[20] and Reed.[21]

The electronic measurements of drag, trim and pressure were recorded digitally and processed by an Interdata computer system mounted on board the towing carriage. A second similar computer system was used to record the longitudinal wave-cut data. The results of the experiments are presented and compared to the analytical predictions of Dawson and Chang in Figures 2 through 21.

It should be noted that the analytical predictions have been made using a discretization technique which assumes that the various hydrodynamic quantities are constant on each panel. Therefore, small spatial variations cannot be predicted if they occur over distances smaller than the local panel dimension. When the location of an experimental measurement did not coincide with the centroid of a panel, the measurement was compared to the predicted value at the nearest centroid, or, in some cases, a linear interpolation between the two nearest centroids. Also, for clarity in presentation, all experimental values are shown as discrete point symbols while all predictions are shown as continuous lines drawn through the predicted values at the center of the panels. Nevertheless, it should be kept in mind that the predictions, as well as the measurements, are actually discrete points.

Because of the important connection between running trim and drag for high-speed ships, as pointed out by Dawson[17] and Chang,[18] two complete sets of experimental data were obtained. The first was with the model locked to the carriage so that no trim occurred at any speed. The second was with the model mounted to counterbalanced pivots so that it was free to trim under the action of the hydrodynamic force and moment generated by its forward speed.

RESULTS

DRAG

The results of the drag measurements and predictions for the two conditions of trim are presented in Figures 2 and 3. All results are shown as nondimensional drag coefficients as a function of length Froude number (F_n). Experimental values are shown for both residual (C_R) and wave (C_W) drag coefficients, although predictions are available only for the wave drag coefficient. Total drag was measured at a large number of speeds in order to accurately define the shape of the resistance coefficient. The measurement of drag with the floating girder, when corrected for the air drag of the girder and supporting struts, was found to agree closely with the measurement from the force block. The residuary drag coefficient was calculated from the total drag coefficient using the 1957 ITTC model-ship correlation line. The parasitic drag of the trip wire was calculated with an assumed drag coefficient of 0.6 (based on the frontal area of the trip) and the residuary resistance coefficient curves shown in Figures 2 and 3 have been corrected for this parasitic drag.

8

Experimental values of wave drag coefficient, as determined from analysis of the longitudinal wave cut data, are shown for $0.20 \leq F_n \leq 0.50$, although predictions were made only for $F_n \geq 0.31$ for the reasons mentioned previously. As can be seen, the wave drag coefficient is roughly parallel to the residuary coefficient, and the predicted values of C_W generally agree well with the measured values. The C_R curve for the free-to-trim condition is significantly greater than the C_R in the zero trim condition at all speeds, with the difference between them increasing at high speeds. At a Froude number of 0.50, the highest test speed, the C_R in the free-to-trim condition was 36 percent greater than the corresponding value without trim. The data for wave drag are generally closer for the two trim conditions at low speeds, while for a Froude number of 0.40 or greater, the C_W curves for the two conditions deviate in a way similar to the C_R curves. The most obvious deviation from the trends discussed above is at the highest speeds with the hull free to trim. Here, the difference between the measured C_R and C_W curves is noticeably greater than at lower speeds, and the predicted values of C_W are lower than the measured values.

Figure 4 presents a "worm curve" showing the ratio of the total resistance of this transom stern hull (free to sink and trim) to that of a Taylor Standard Series hull having the same overall hull proportions. This illustrates the usual trend for such a hull. That is, it has inferior drag at low speeds ($R_T/R_{T_{Taylor}} > 1.0$), roughly comparable drag at intermediate speeds ($0.30 < F_n < 0.40$) and superior drag at higher speeds. This trend is expected to be exaggerated for a full-scale ship, where the frictional drag penalty caused by the increased wetted surface of a wide transom stern will be relatively less, because of the reduced frictional coefficient at high Reynolds number.

TRIM

The change of level at bow and stern is shown in Figure 5 for the free trim condition. The results are nondimensionalized by hull length. The experimentally measured values at both bow and stern show gradually decreasing (sinking) values up to $F_n = 0.34$, indicating primarily a level sinkage with little trim from bow to stern. As speed is increased beyond this point, the bow begins to rise while the stern sinks at an increasing rate. The measured stern sinkage at $F_n = 0.50$ is so

9

great that the draft of the transom is approximately five times its static draft.
The predicted change of level at the stern generally shows satisfactory agreement
with the measured values. The change of level at the bow predicted by the XYZFS
program does not agree so well with the measurements, while the predictions from the
Chang program are in better agreement except near the highest Froude numbers.

The data in Figure 5 may help to explain some of the trends in the C_R and C_W
curves shown in Figures 2 and 3. For instance, the C_R curve is greater in the free
trim condition than in the zero trim condition, even at low speeds where wavemaking
drag is small. This apparent increase in residuary resistance may actually be
frictional resistance of the increased wetted surface associated with the level sink-
age shown in Figure 5. Also, the change in both C_R and C_W when the hull is allowed
to trim at high speed appears to be directly related to the increased hydrostatic
drag of the trimmed transom, as hypothesized by Chang.[18]

PRESSURE

The results of the pressure measurements, and predictions from the XYZFS program,
in the fixed and free trim conditions are shown in Figures 6 and 7, respectively.
The results are shown for five Froude numbers and at two transverse locations:
centerline, and a line parallel to the centerline but offset a distance equal to
two-tenths of the maximum beam. The data are represented as nondimensional dynamic
pressure coefficient (C_P) values, defined as:

$$C_P = \frac{p - \rho g h}{\frac{1}{2}\rho V^2}$$

where h is the static depth of a particular pressure tap (including any trim). This
is considered a reasonable assumption for the speeds in question, since the transom
was dry and the flow broke cleanly from the corner of the transom, forming a jet at
the free surface. It can be seen that the XYZFS predictions indicate very little
variation in pressure in the transverse direction. In the axial direction the C_P
is generally predicted to rise from a small negative value at station 17, rising to

10

near zero around station 19, then dropping rather sharply toward the transom. This last trend is a consequence of the fact that the pressure at the transom must be atmospheric. Therefore, the pressure coefficient should reach a final value,

$$C_P = -\frac{2gh}{V^2}$$

at the transom, where h is the draft to the bottom of the transom, including any trim effects. This limiting value of C_p is shown as an asterisk (*) at station 20 in Figures 6 and 7.

The measured pressures were found to contain considerable scatter, even when measuring hydrostatic pressure on the hull at zero speed. This is believed to be caused partly by leakage of air in the manifold and valve system, and partly by the very low pressure levels measured. The pressure transducer used was rated at 5 psi (34,474 Pa) full scale in order to be compatible with the air pressure required to purge water from the tube system. The measured pressures on the hull were generally of the order of 0.1 psi (690 Pa) or less. Therefore, the measured pressures were near the minimum resolving ability of the pressure measurement system, resulting in a large amount of scatter. In view of the limited accuracy of the pressure measurements, it can be said that the predicted and measured pressures are in general agreement, and both follow the proper trend as the transom is approached. The largest difference between the predicted and measured pressures is at the highest speeds in the free trim condition, where there is a considerable discrepancy from station 18 to station 19 1/2.

WAVE PROFILES

Figures 8 and 9 show comparisons of predicted and measured wave profiles along the side of the hull for the zero and free trim conditions, respectively. Predicted values from the XYZFS program are presented for all five Froude numbers at both zero (fixed) and free trim conditions. Predictions from the Chang program are available for four of the Froude numbers at the zero trim condition. The elevations are presented relative to the calm water free surface level, and are nondimensionalized b hull length.

11

For the zero trim case shown in Figure 8, the magnitude and shape of the predicted curves agree well with the measured values, especially at the lower Froude numbers. There is a kink in the XYZFS predicted bow wave profiles at all speeds which is more pronounced at higher speeds. This is not apparent in the Chang predictions or in the experimental data, which is smoother. The predicted local wavelength by Chang appears in Figure 8 and it seems to be off somewhat, as reflected in the wave profile zero crossing occurring downstream of the measured location and that predicted by the XYZFS program. In the free-to-trim case shown in Figure 9, the agreement is not as good. At all Froude numbers the experimental bow wave height is higher than the predicted values. The kink in the predicted bow wave profile is still apparent on the free trim plots. At the stern, the experimental values agree fairly well with the XYZFS predicted values except at Froude numbers of 0.45 and 0.50 where the predicted results were far off scale from station 19 aft. At $F_n = 0.45$ and more so at $F_n = 0.50$, the XYZFS predicted results are not as smooth as the experimental results along the length of the entire model.

STERN WAVE ELEVATIONS

Figures 10 through 14 show the measured and predicted wave elevations aft of the hull for the zero trim condition at five Froude numbers, while the free trim condition is presented in Figures 15 through 19. The axial locations at which measurements were made have been defined in terms of the same station numbering system used for the hull. For example, the first measurement location behind the transom was at station 20 1/2, which is one-fortieth of the hull length behind the transom. The experimental measurements are plotted at each place where the data were taken, whereas the theoretical predictions were interpolated to correspond to the stations at which the experimental data were taken. Those theoretical values were then faired in a smooth curve as is shown in the figures.

For the fixed trim cases the agreement is fairly good between experimental and theoretical values. The theoretical predictions form a much smoother line than the experimental data, in most cases, smoothing out the humps and hollows of the measured results. The order of magnitude of the experimental results is the same as the predictions.

In the free trim cases of Froude numbers 0.31 and 0.34 shown in Figures 15 and 16, the agreement at all stations is as good as in the fixed trim cases. However, at the Froude number of 0.40, shown in Figure 17, the agreement is not as good. Close to the centerline at station 20 1/2 the predicted results show a slight oscillation, and at stations 22 1/2 and 23 1/2 a larger discrepancy appears especially directly behind the transom.

In the free trim cases of Froude numbers 0.45 and 0.50, shown in Figures 18 and 19, the scale of the graphs is expanded in order to fit both sets of results on the same graph. There are order of magnitude differences between the theoretical predictions and the experimental results, with the worse discrepancies being at stations 20 1/2 and 21 1/2 where even the shapes of the curves are very different.

The shape of the free surface near the transom was also recorded photographically. The results are shown in Figures 20 and 21. The photographs show the flow pattern starting at a Froude number of 0.20 in order to illustrate the qualitative variation as the speed is increased through the range where the transom becomes dry. In the fixed zero trim condition (Figure 20) at Froude number of 0.20 and 0.24, the transom is wetted and the flow directly behind it is a highly irregular, separated flow. At a Froude number of 0.26, the transom is dry, and there is a broad, crescent-shaped breaking wave front directly behind it. At higher speeds, this breaking front is swept aft over the crest of a pyramid-shaped wave crest which becomes prominent at a Froude number of 0.34 and above. As $F_n = 0.50$ is approached, the wave crest behind the transom moves aft and is elongated, and the breaking wave front is swept back into a V-shaped spray sheet (often referred to as a "rooster-tail" wake). For the free-to-trim case (Figure 21), the behavior near $F_n = 0.26$ is nearly identical, since very little change in level has occurred at the transom at that speed (see Figure 5). The behavior of the free surface at higher speeds is also qualitatively similar to the zero trim case, with the exception that the large trim developed results in a deep trough with nearly vertical transverse slope directly behind the transom.

13

DISCUSSION

Th measurements of wave drag (as determined by wave-cut analysis), wave eleva-
tions and pressures on the hull, when fixed at zero trim, indicate that both poten-
tial flow computer programs give reasonable predictions for this condition. The
XYZFS program produces more detailed output, and therefore a more detailed correla-
tion is possible. The XYZFS program also produces an accurate prediction of trim at
the transom at high speeds, while Chang's program somewhat underpredicts this trim.
The predictions of wave drag when the hull is free to sink and trim, whether done by
the iterative repaneling scheme of the XYZFS program or simply by the increased
hydrostatic drag hypothesized by Chang, are quite similar. However, both programs
underpredict the wave drag at high speed in the free trim condition. Furthermore,
details of the flow predicted by the XYZFS for the high-speed, free trim condition
are noticeably different from the measured values. Predicted wave elevations along
the side of the hull tend to oscillate and then diverge as the transom is approached
at F_n = 0.45 and 0.50, and predicted wave elevations behind the transom also do not
agree well with the measurements. It is possible that these problems are caused by
an inadequate spatial resolution (panels too large) near the transom. Spatial
resolution may also have a bearing on the predicted kink in the bow wave profile,
which was not substantiated in the experiments, and certainly must be increased if
predictions are to be made for Froude numbers lower than those considered in this
report. Another probable source of difficulty in calculating the flow at high speed
(particularly with free trim) is that the actual flow is in the form of a deep cavity
behind the transom, with nearly vertical slopes in some places, and this cannot be
expected to satisfy a linearized free surface boundary condition.

The measured residuary drag coefficient (C_R) is considerably higher than the
wave drag coefficient (C_W) over the entire speed range covered in the experiments,
for both zero trim and free trim conditions. The difference between C_R and C_W also
increases at higher speeds. Because frictional resistance is normally estimated
with the static wetted surface, a calculation was made of the increased frictional
resistance expected due to the dynamic wetted surface (a combination of wave profile
and trim effects). This calculation indicated that the dynamic wetted surface effect
could account for most of the increasing difference between C_R and C_W at higher
speeds. However, it appears that a substantial form drag component still exists

14

which cannot be accounted for by either free surface potential flow or flat plate friction calculations. Breaking waves were observed at both the bow and stern in the experiments, and in addition a considerable amount of spray was generated, particularly in the free trim condition. Also, at lower speeds there was obviously a separated flow region behind the transom. It is difficult to quantify these effects, but each may be the source of the form drag in different speed ranges.

The potential flow calculations were made only in the range $0.31 \leq F_n \leq 0.50$, and the transom was observed to be dry over this entire speed range. The transom was observed to become dry at a Froude number of 0.26. Calculations at this speed would probably require an increased number of panels. However, neither computer program has a capability of predicting the speed at which the transition from a wetted to a dry transom occurs, since this phenomenon appears to be a complicated interaction between viscous and nonlinear free surface effects. This transition speed corresponds to a Froude number, based on transom centerline draft, of 4.14, which agrees with the value recommended by Saunders[6] for determining transom depth. This Froude number is considerably higher than the value of 2.23 predicted by Vanden-Broeck[13] and Haussling[14] as the minimum depth Froude number at which steady state waves can exist behind a two-dimensional transom. However, it is important to note that at a Froude number of 0.26, where the transom becomes dry, the drag of this hull is still considerably higher than an equivalent Taylor Standard Series hull, and the favorable drag associated with a transom stern is only achieved at much higher Froude numbers.

CONCLUSIONS

Free surface, source-distribution potential flow computer programs have been found to give reasonable predictions for the wavemaking drag component of a transom stern hull form. The importance of sinkage and trim, and the hydrostatic drag component due to a dry transom, as pointed out by Dawson[17] and Chang,[18] has been confirmed. However, the correlations reported here are for only one hull form, and further correlations are recommended. Furthermore, there are several questions regarding the accuracy of the computations at the highest Froude number considered ($F_n = 0.50$) and further investigation of the details of the numerical predictions, particularly near the transom, is needed.

15

Methods for predicting other components of drag associated with transom flow do not exist. The total drag of a transom stern hull may be affected by viscous separation, wavebreaking and spray behind the transom. Each of these effects may make an important contribution to the form drag (the difference between residuary and wave drag) in some speed range. Although the speed at which the transom becomes dry can be predicted by the depth Froude number of the transom, the transition to a dry transom is not necessarily a guarantee that a transom stern hull will have low drag at that speed.

ACKNOWLEDGMENTS
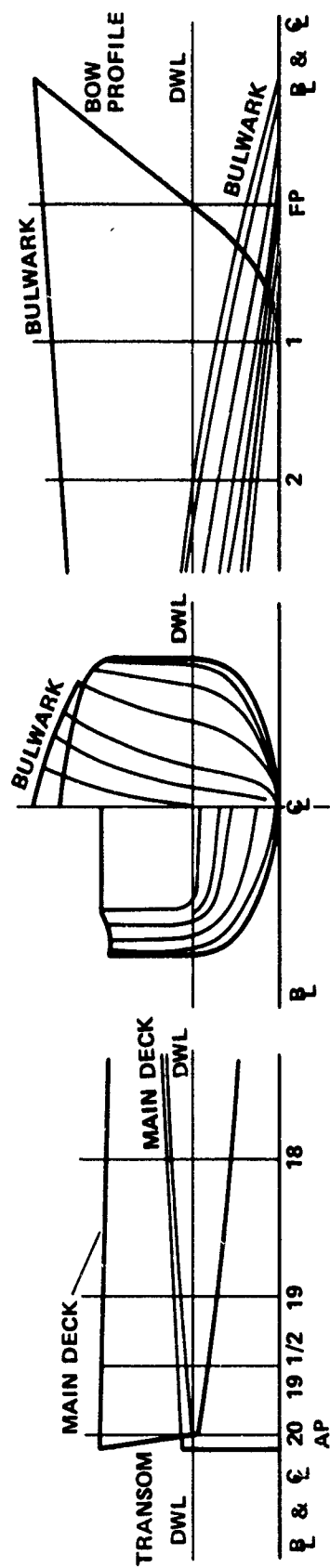
Figure 1 - Abbreviated Lines Plan of Model 5322
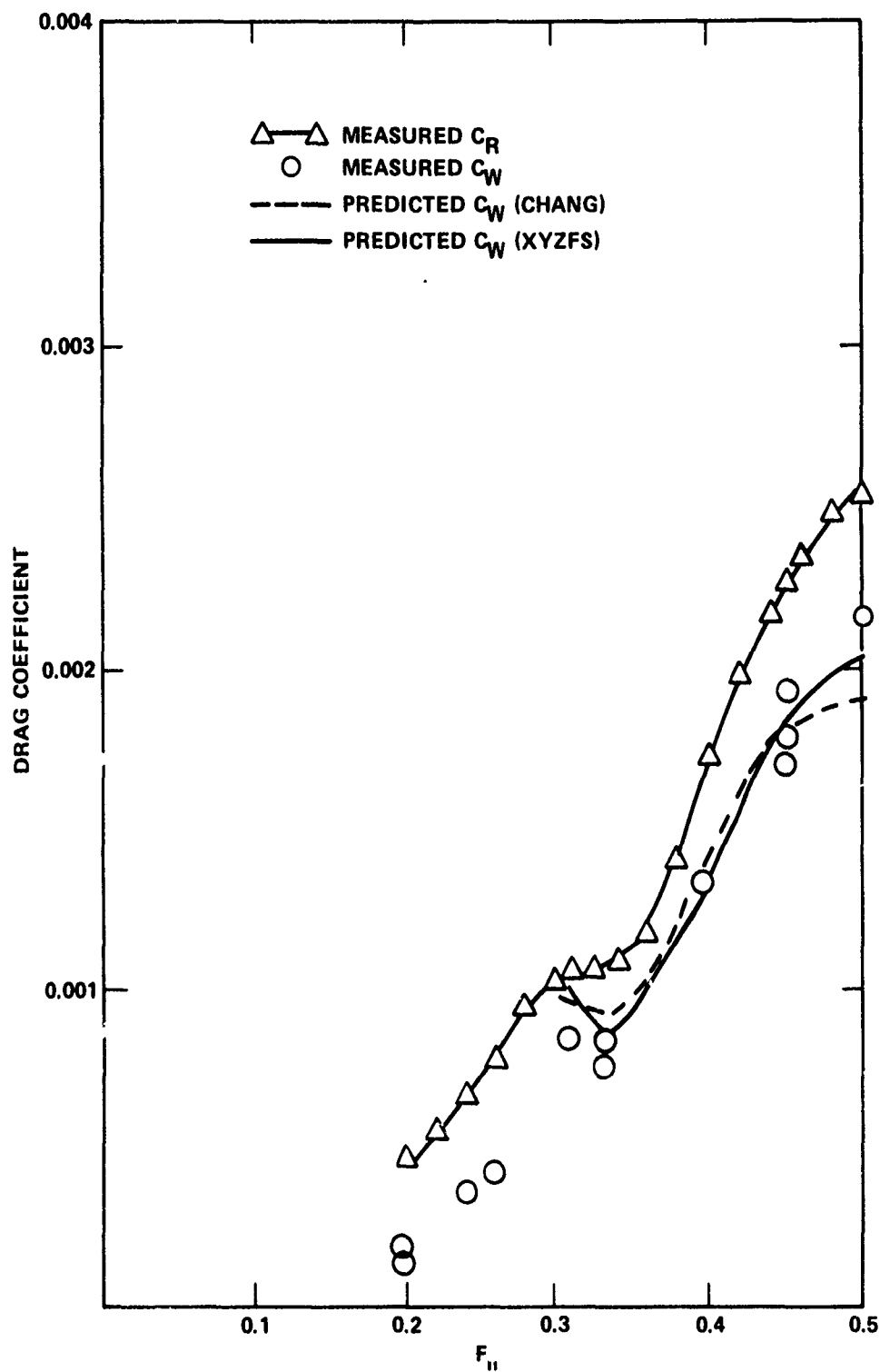
Figure 2 - Comparison of Residual and Wave Drag Coefficients--
Zero Trim

18
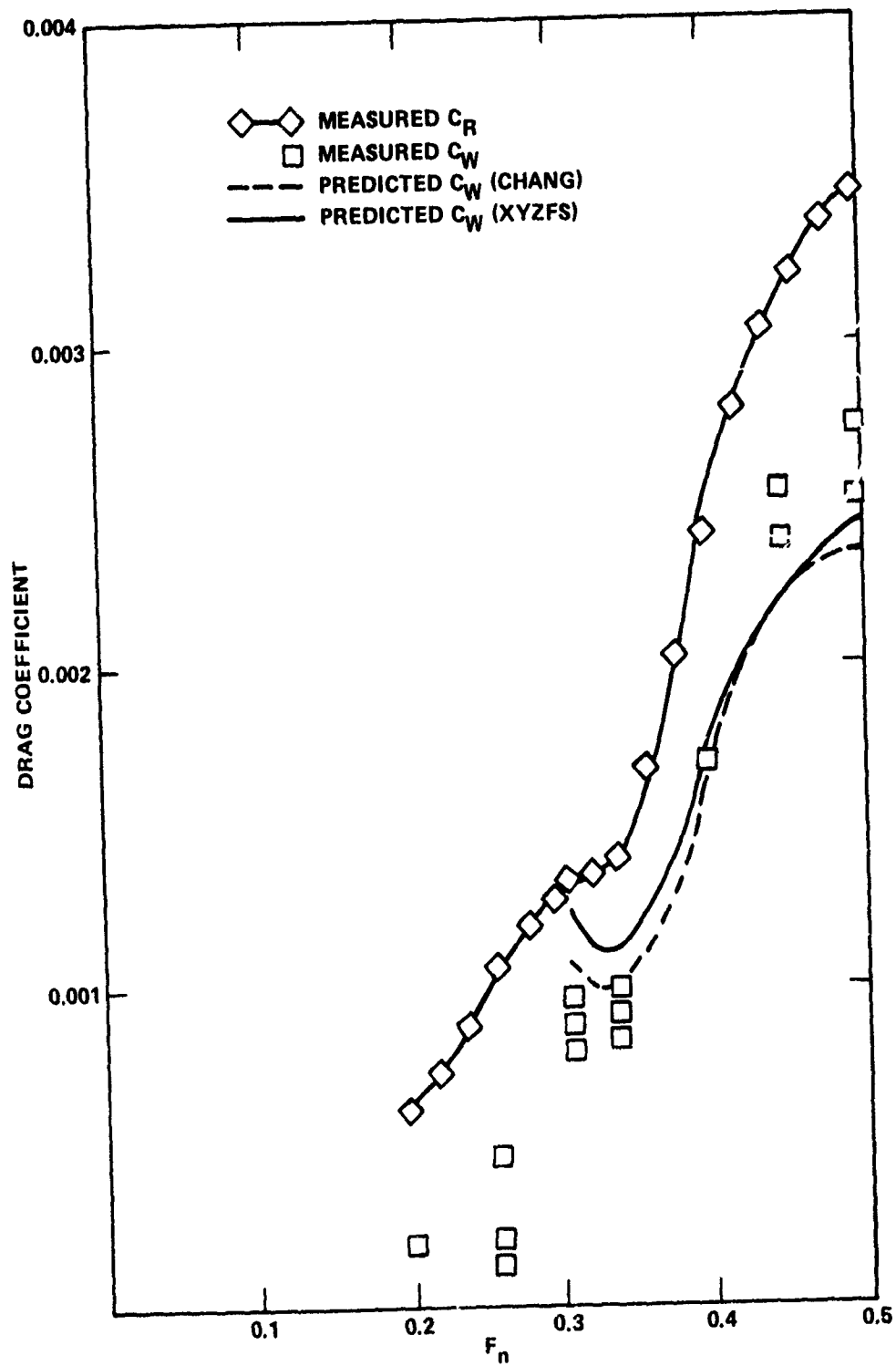
Figure 3 - Comparison of Residual and Wave Drag Coefficients--
Free to Trim
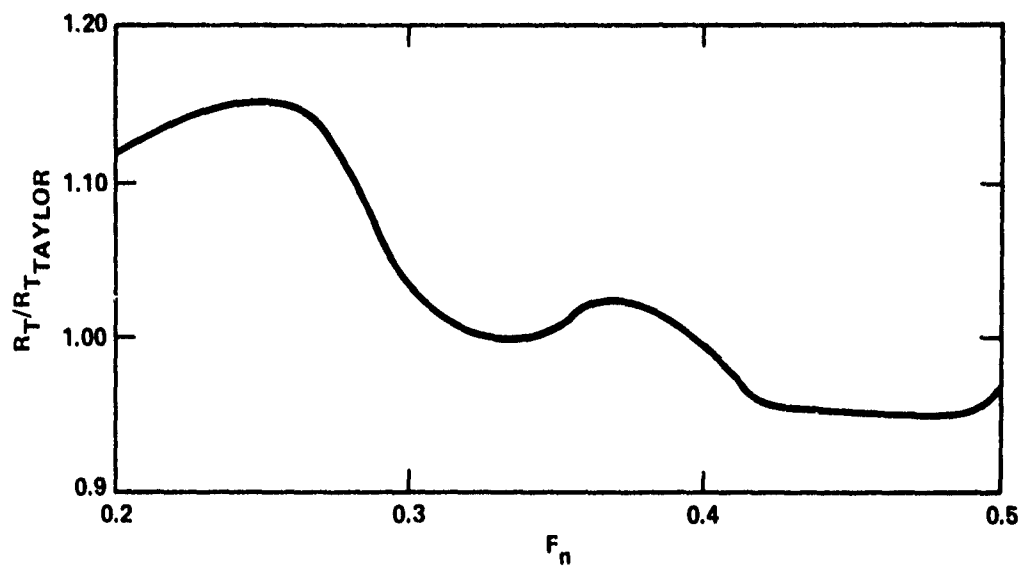
Figure 4 - Worm Curve for Model 5322 Based on Model Length--
Free to Trim
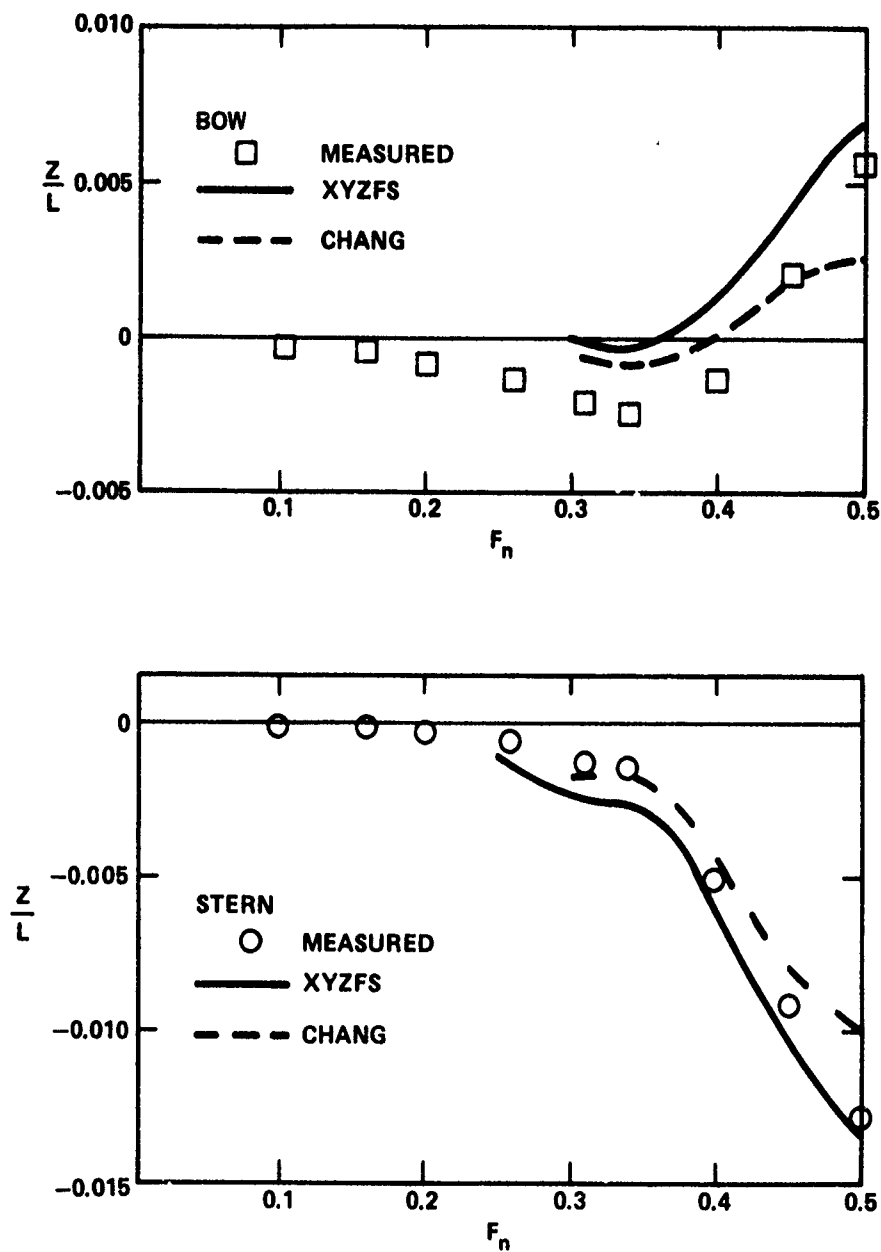
Figure 5 - Comparison of Measured and Predicted Change of
Level (Trim) at Bow and Stern
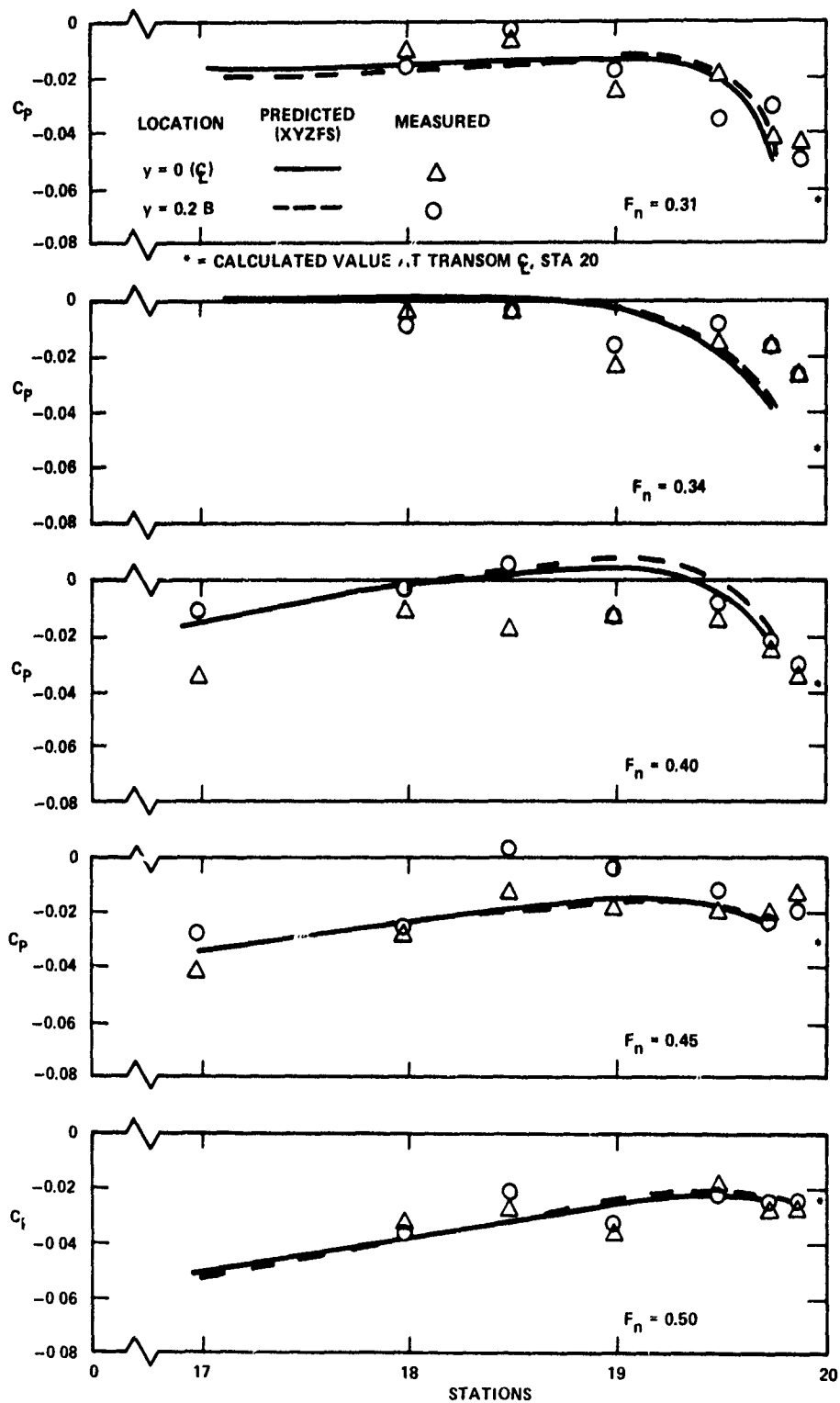
Figure 6 - Comparison of Predicted and Measured Pressure
Coefficients--Zero Trim

22
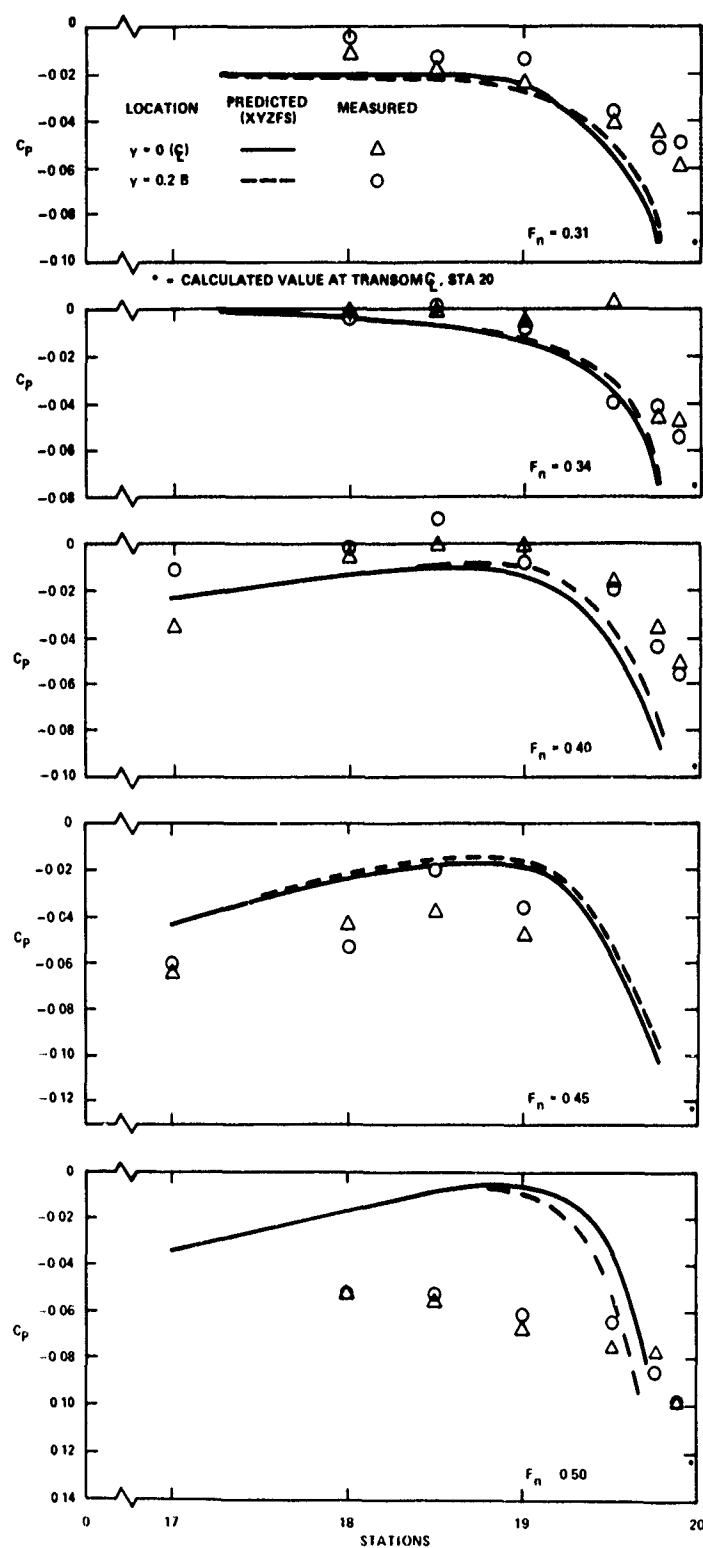
Figure 7 - Comparison of Predicted and Measured Pressure
Coefficients--Free to Trim
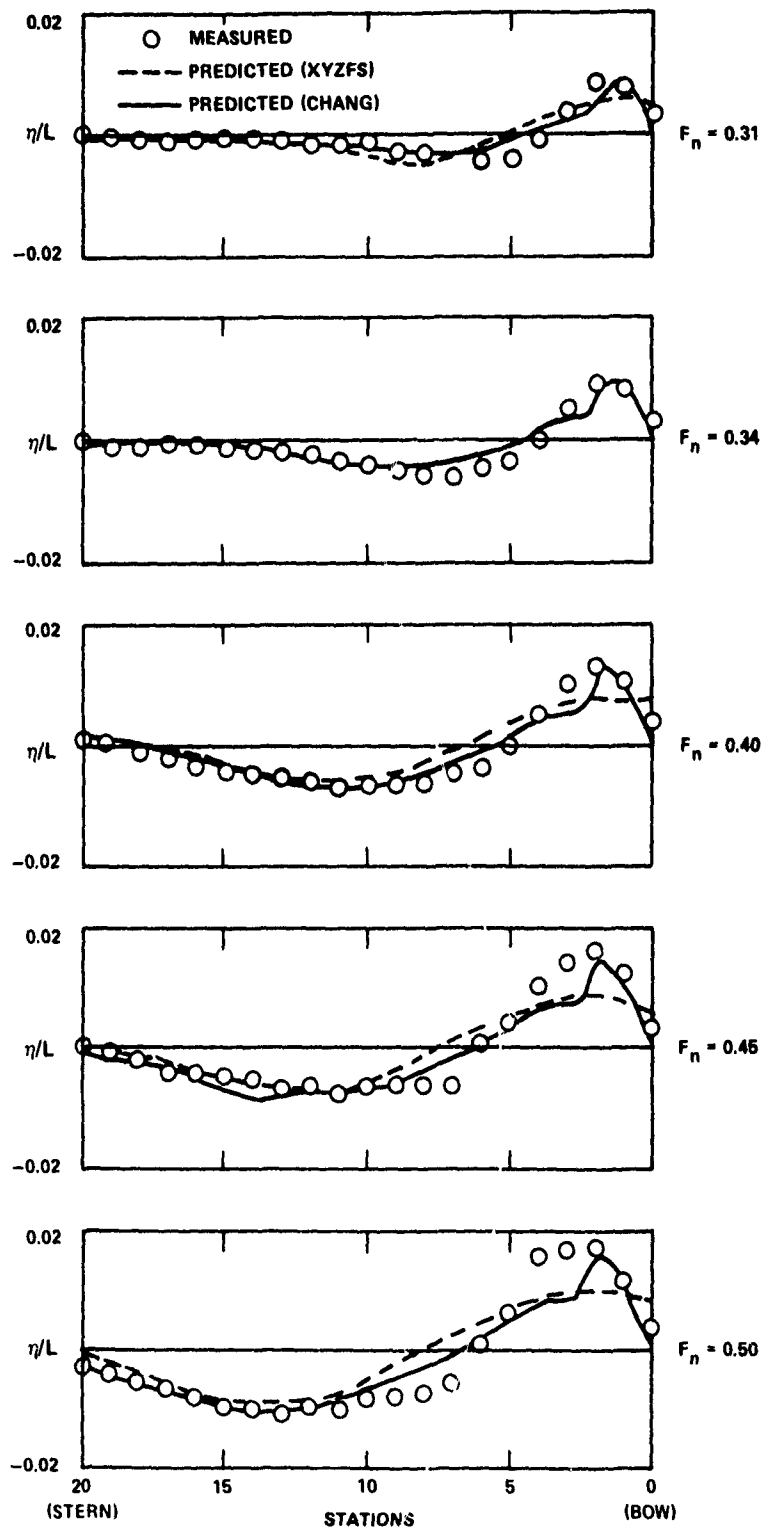
Figure 8 – Comparison of Predicted and Measured Wave
Profiles--Zero Trim

24
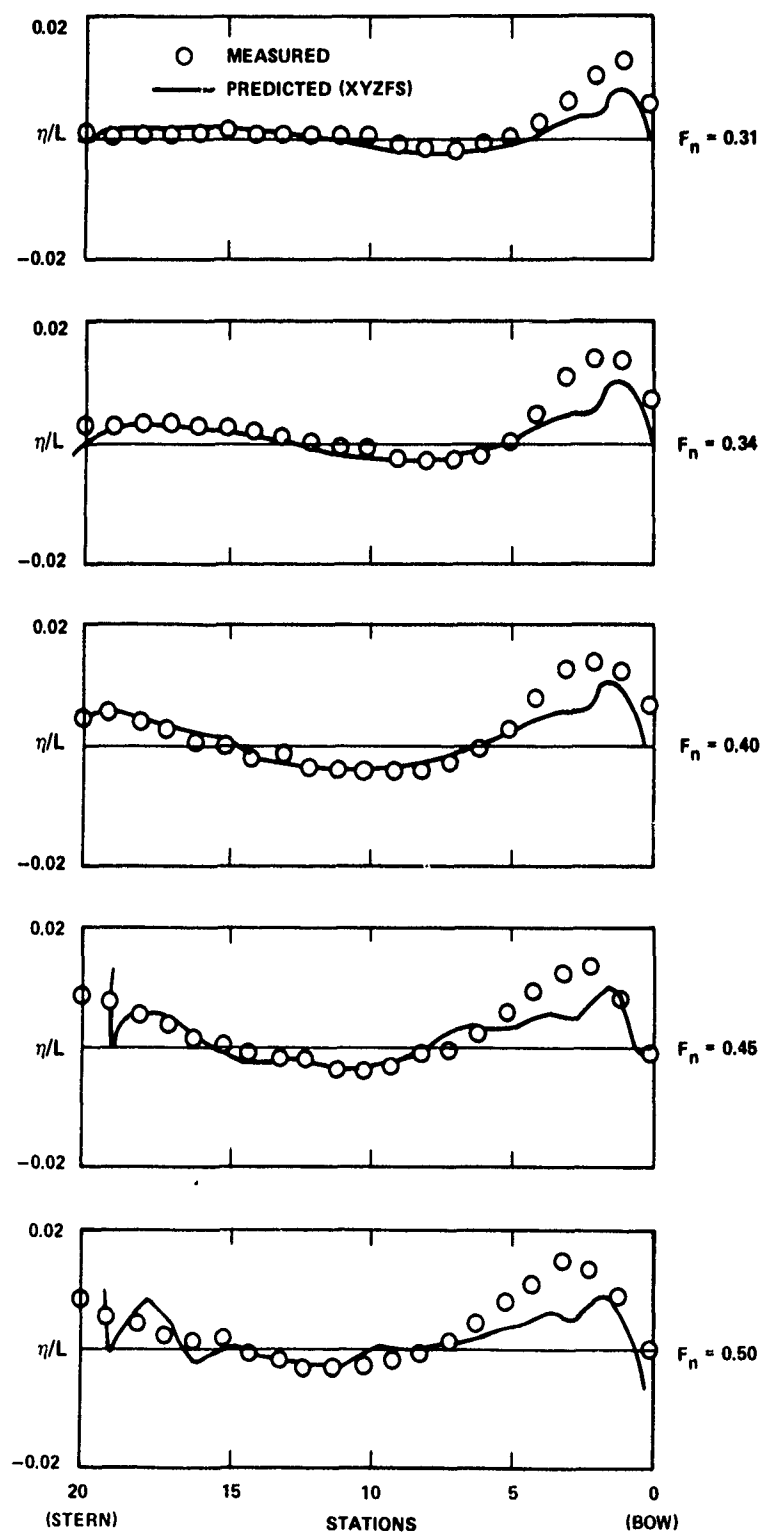
Figure 9 – Comparison of Predicted and Measured Wave
Profiles--Free to Trim
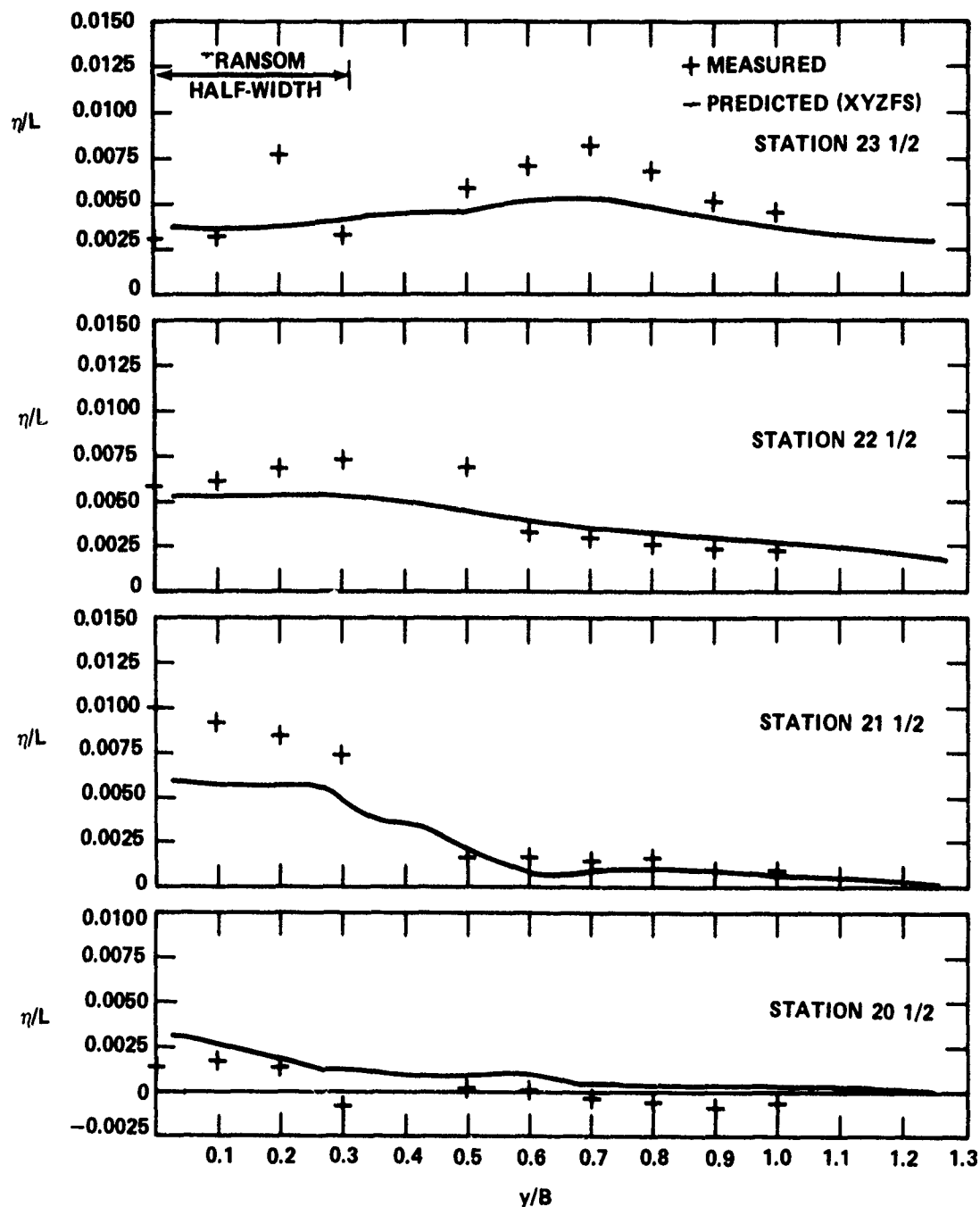
Figure 10 - Comparison of Predicted and Measured Wave Elevations Behind the Transom--Fixed-Zero Trim, $F_n = 0.31$
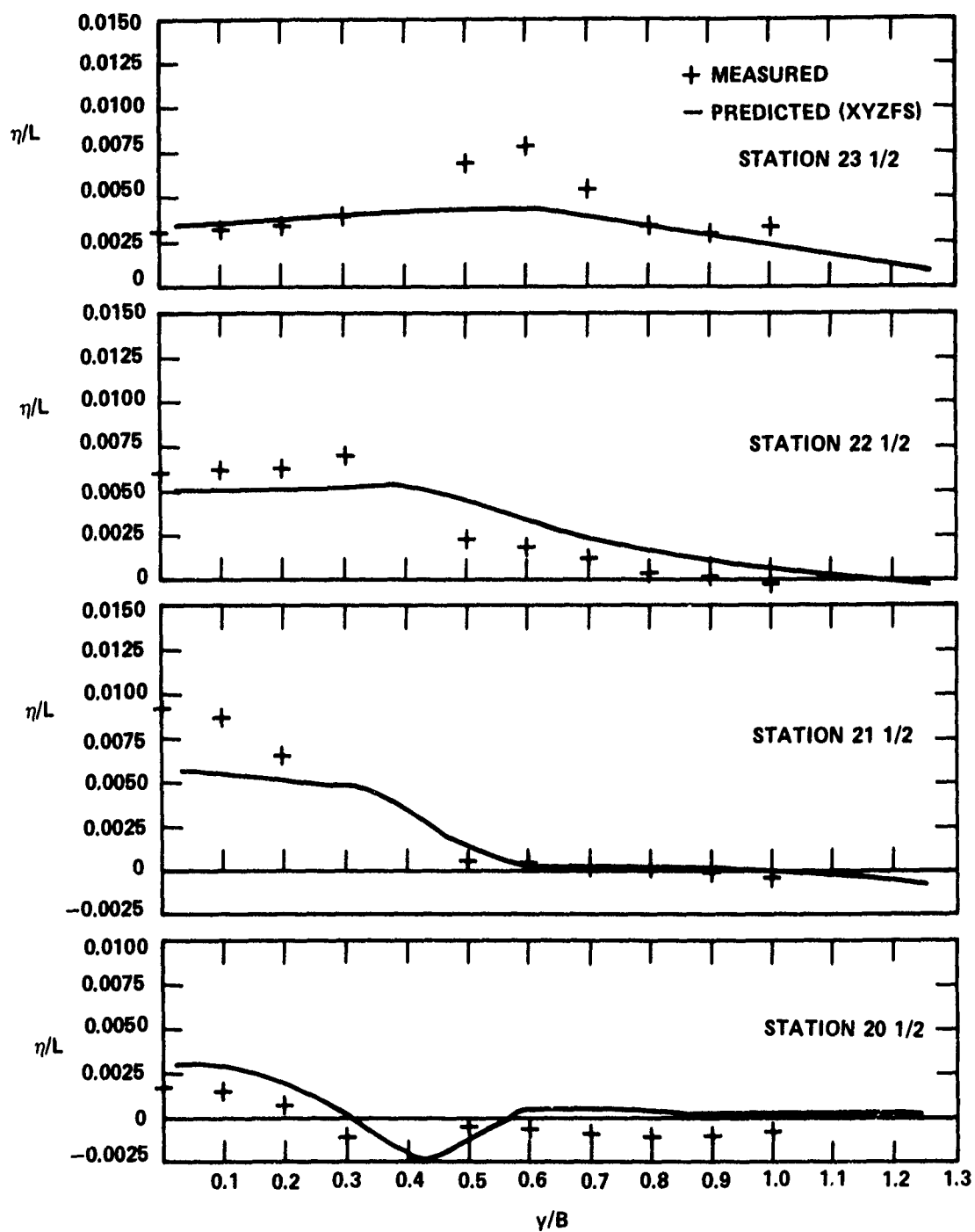
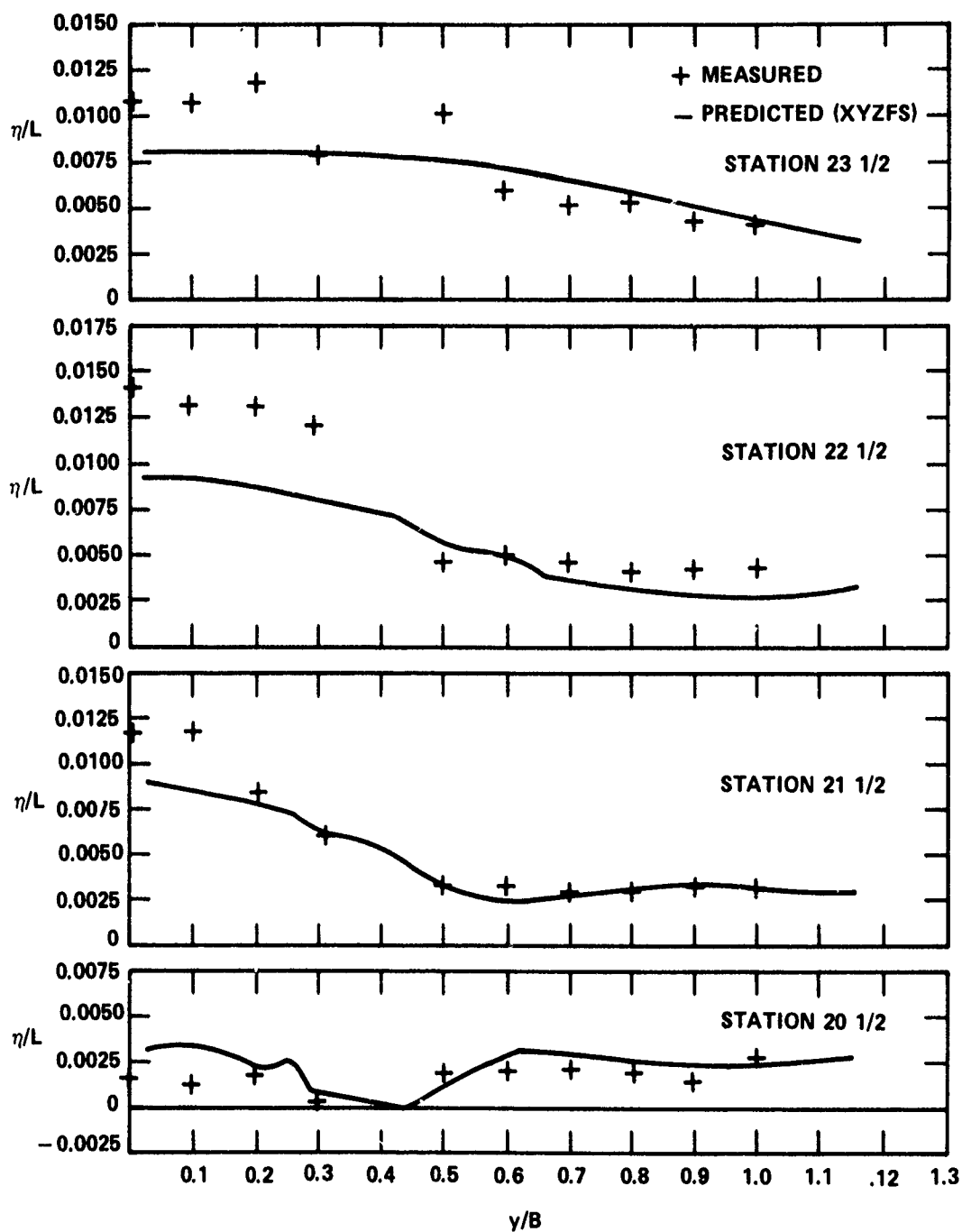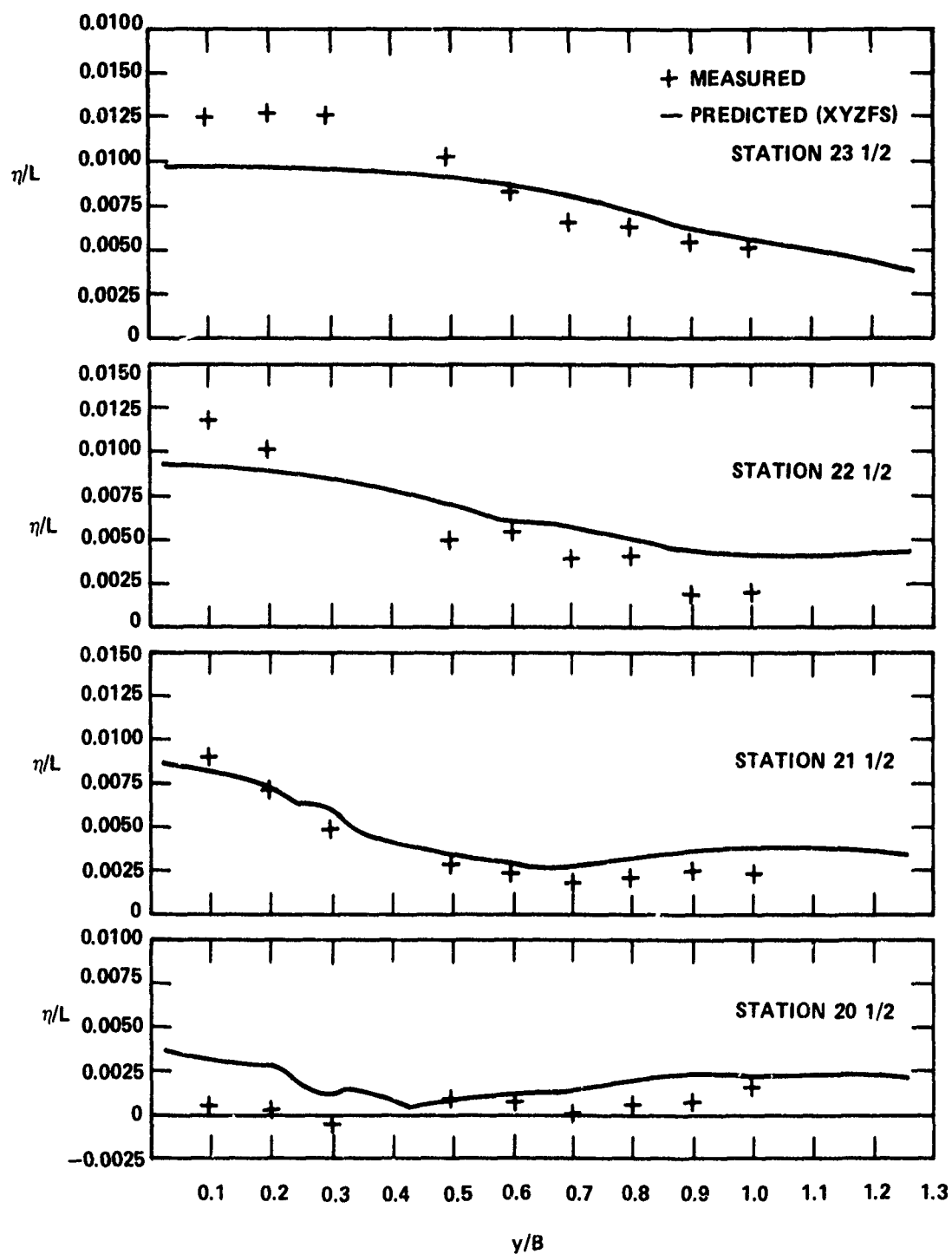Figure 11 - Comparison of Predicted and Measured Wave Elevations Behind the Transom--Fixed-Zero Trim, $F_n = 0.34$

27

Figure 12 - Comparison of Predicted and Measured Wave Elevations
Behind the Transom—Fixed-Zero Trim, $F_n = 0.40$

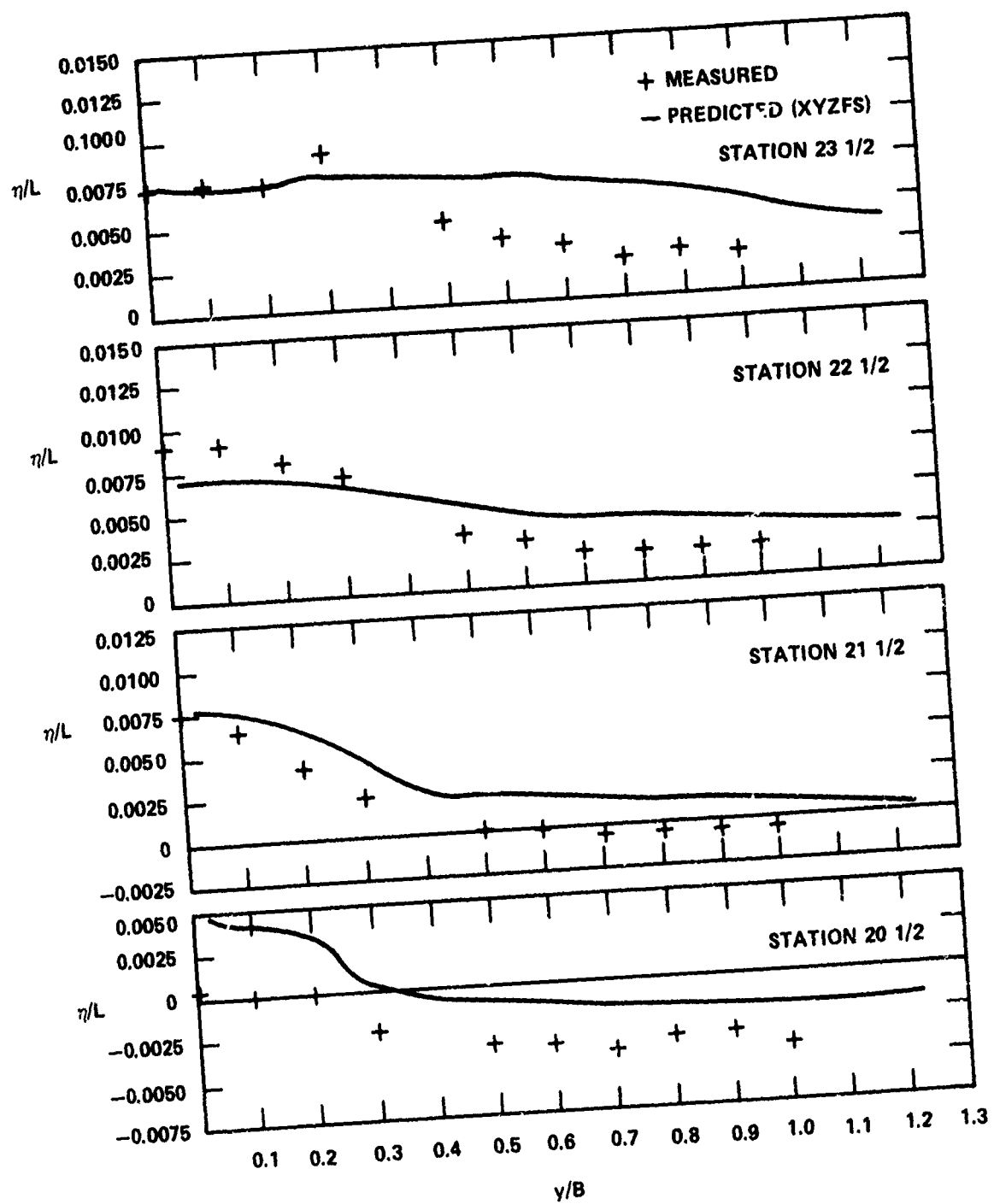Figure 13 – Comparison of Predicted and Measured Wave Elevations Behind the Transom--Fixed-Zero Trim, $F_n = 0.45$

29

Figure 14 – Comparison of Predicted and Measured Wave Elevations
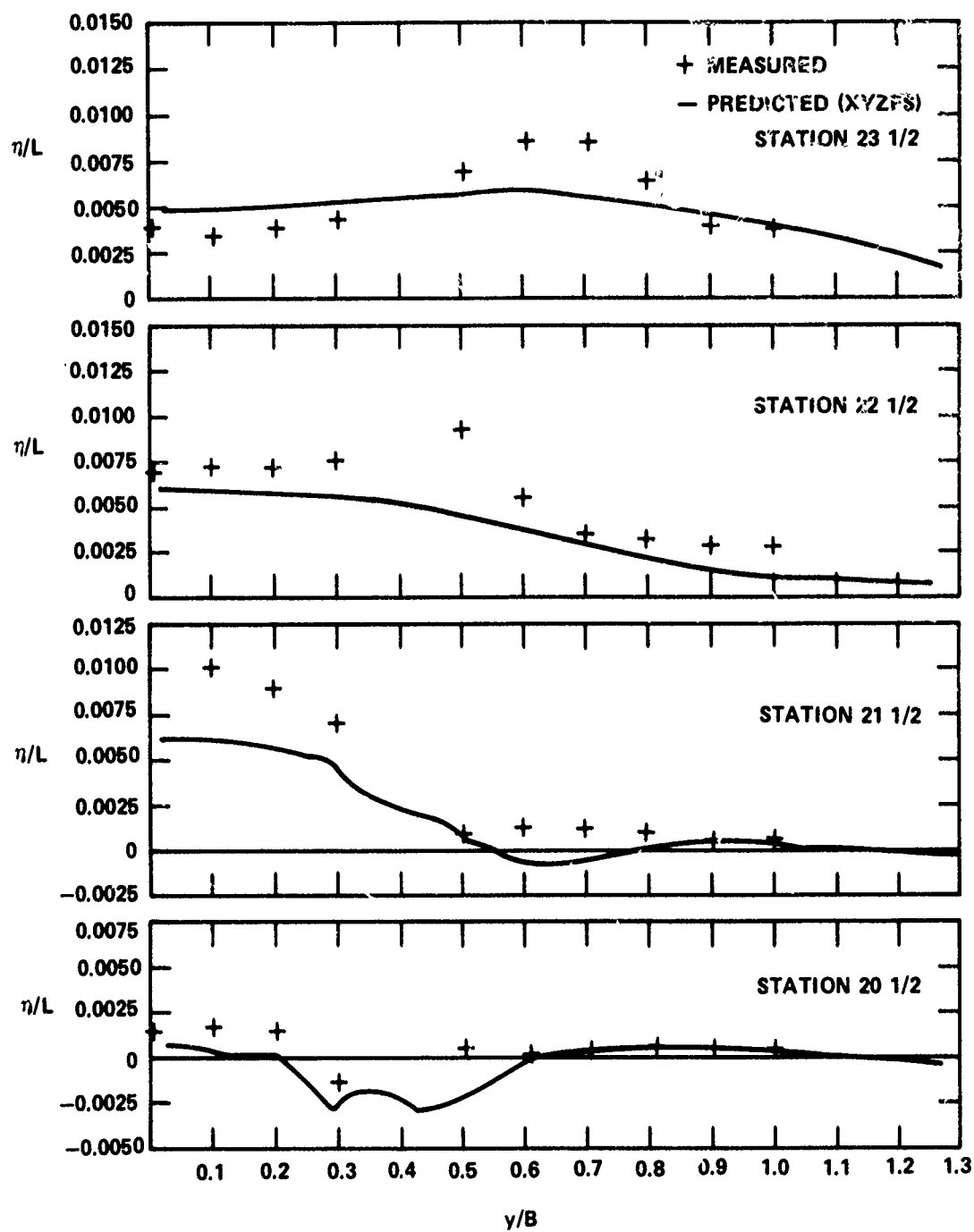Behind the Transom--Fixed-Zero Trim, $F_n = 0.50$

Figure 15 - Comparison of Predicted and Measured Wave Elevations Behind the Transom—Free Trim, $F_n = 0.31$
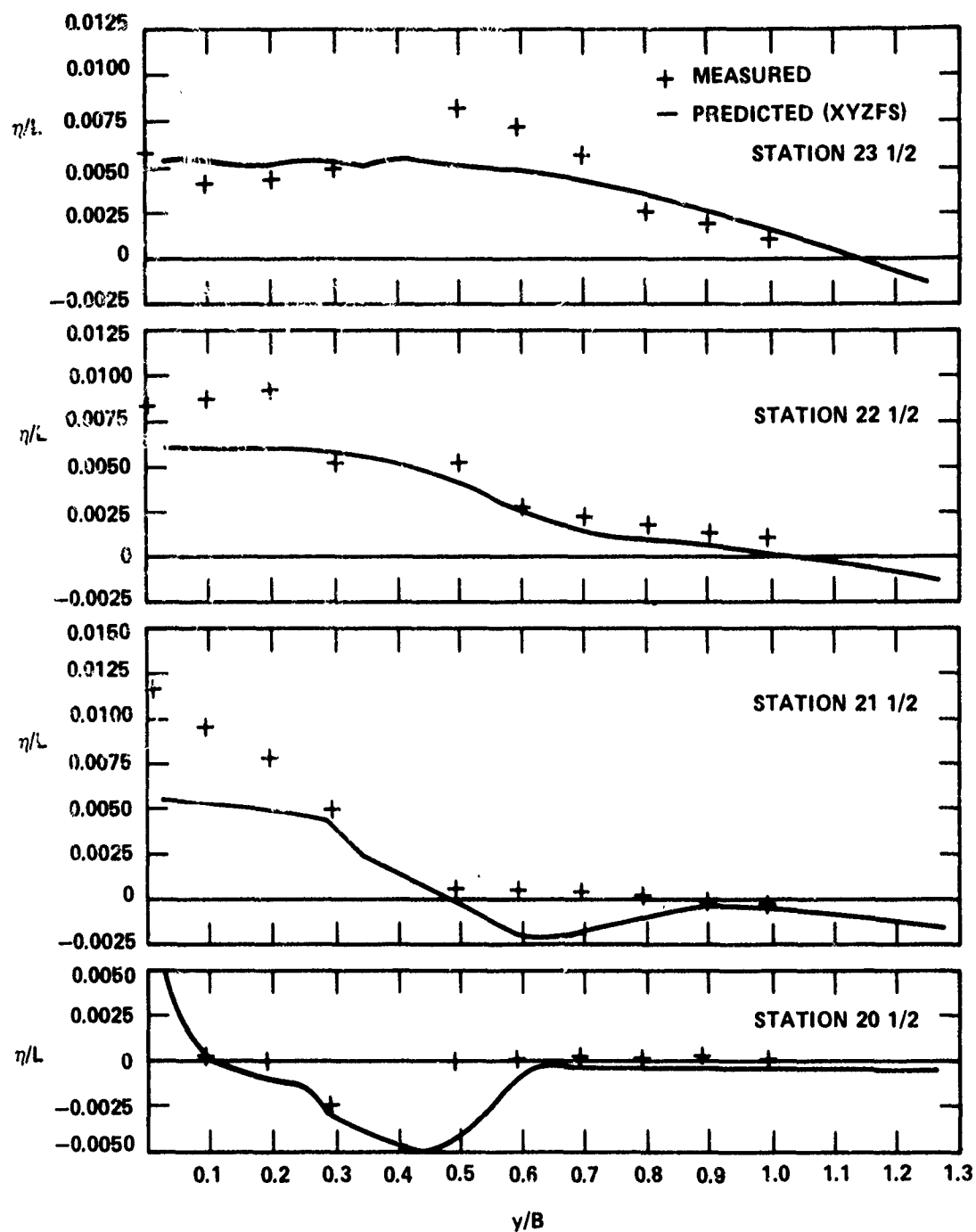
31

Figure 16 - Comparison of Predicted and Measured Wave Elevations
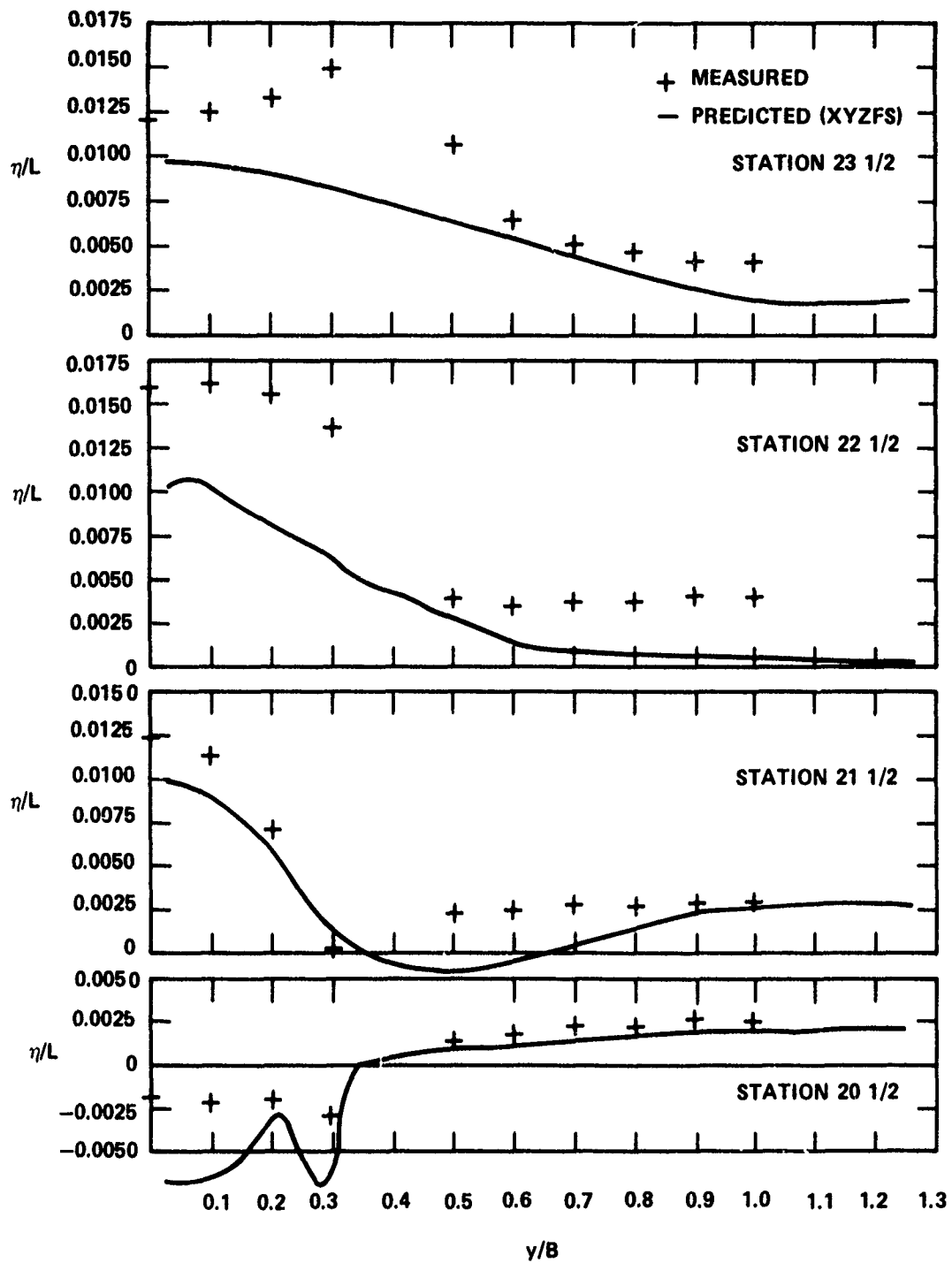Behind the Transom--Free Trim, $F_n = 0.34$

Figure 17 - Comparison of Predicted and Measured Wave Elevations
Behind the Transom--Free Trim, F_n = 0.40
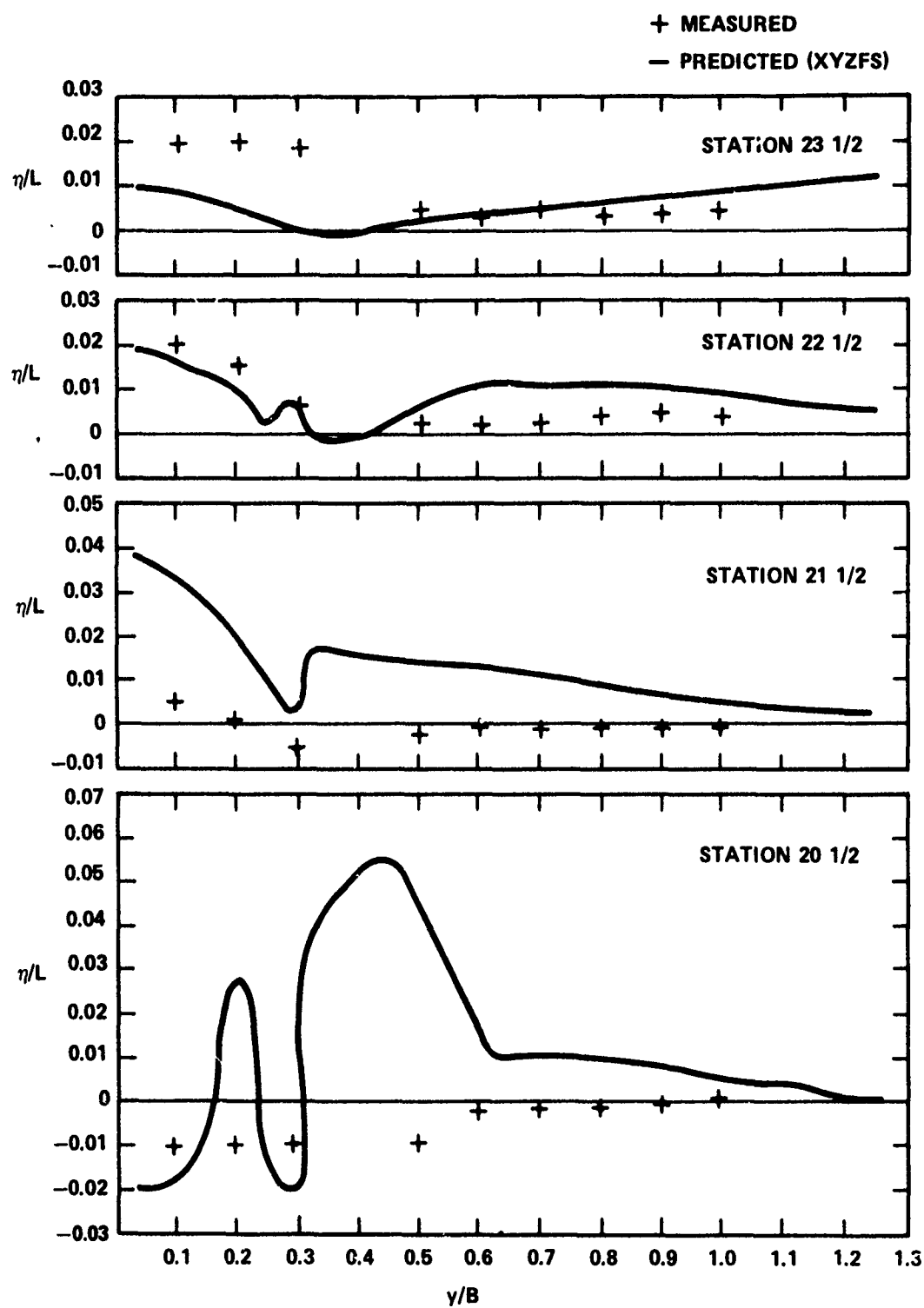
Figure 18 – Comparison of Predicted and Measured Wave Elevations
Behind the Transom--Free Trim, $F_n = 0.45$

34

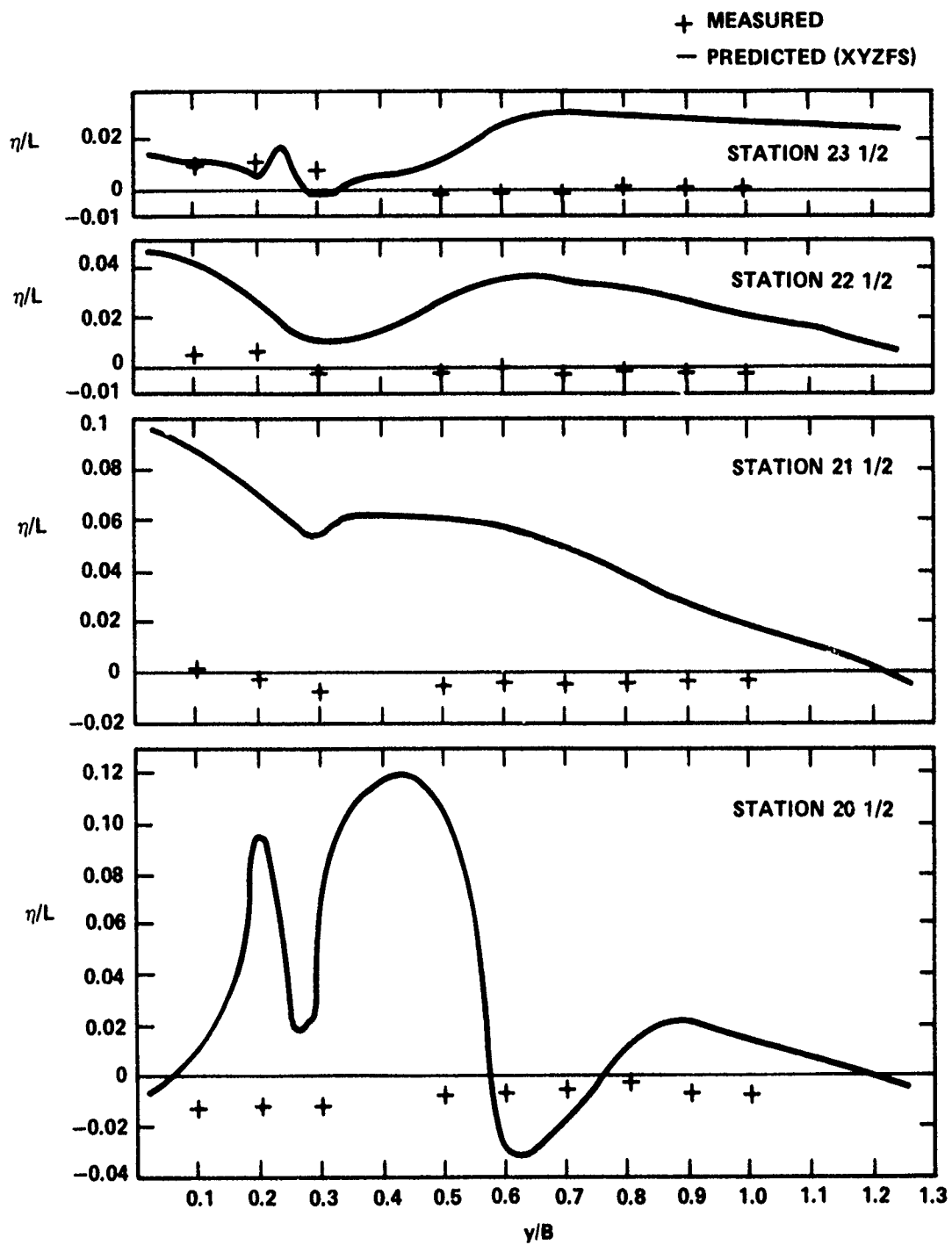Figure 19 – Comparison of Predicted and Measured Wave Elevations Behind the Transom--Free Trim, $F_n = 0.50$

Figure 20 – Flow Near Transom, Zero Trim Condition

Figure 20a – F_n = 0.20

Figure 20b – F_n = 0.24

Figure 20c – F_n = 0.26

Figure 20d – F_n = 0.28

Figure 20 (Continued)
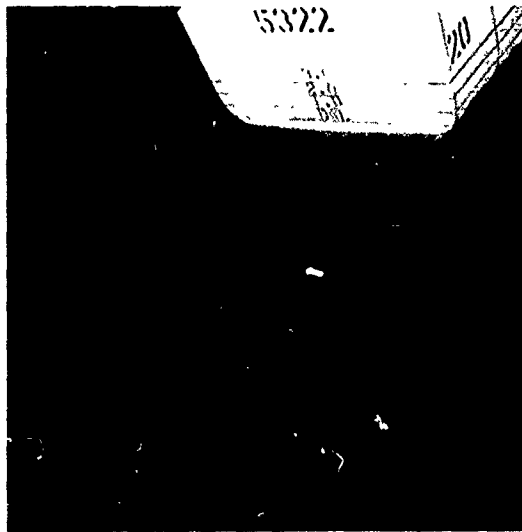
Figure 20e – F_n = 0.34
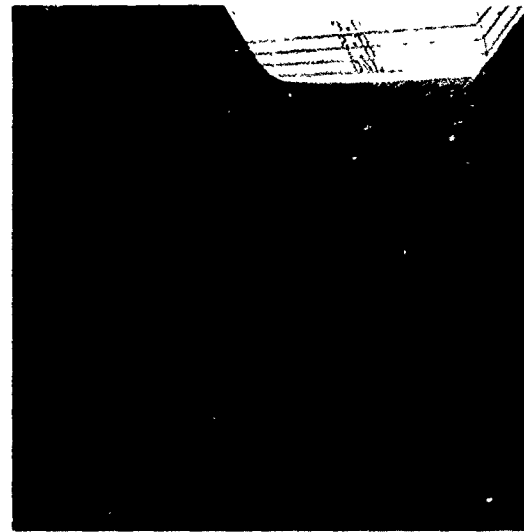
Figure 20f – F_n = 0.40
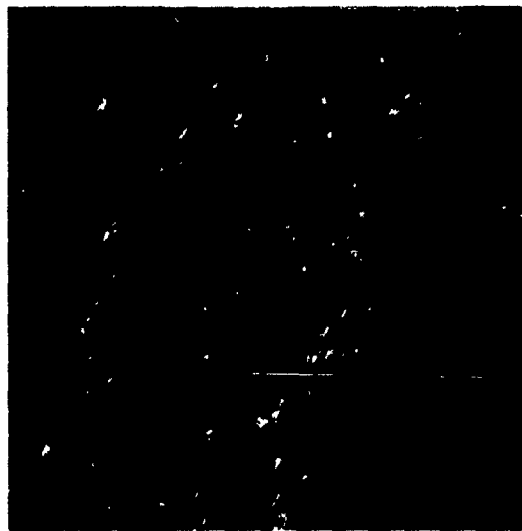
Figure 20g – F_n = 0.45

Figure 20h – F_n = 0.50

Figure 21 - Flow Near Transom, Free Trim Condition

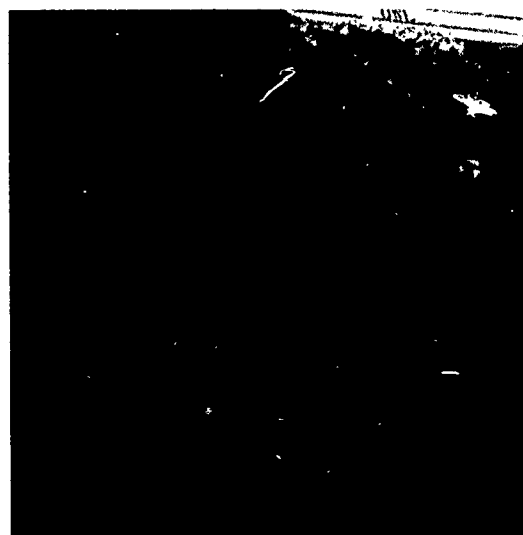Figure 21a - F_n = 0.20
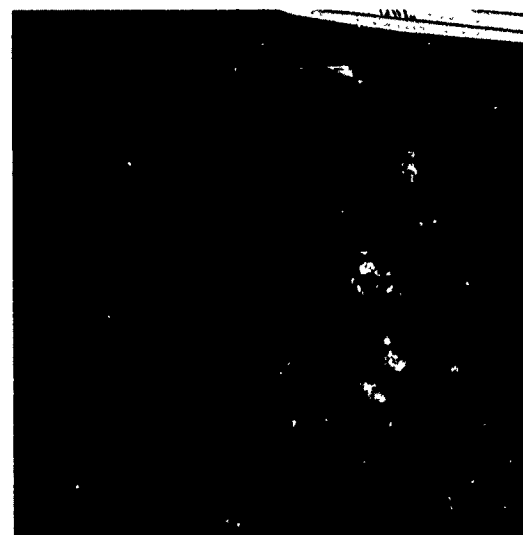

Figure 21b - F_n = 0.24
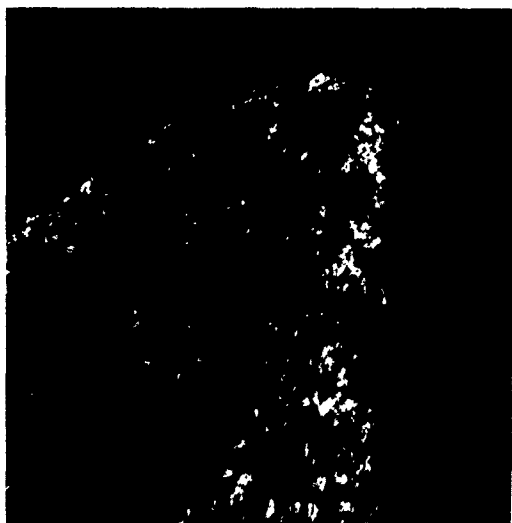
Figure 21c - F_n = 0.26
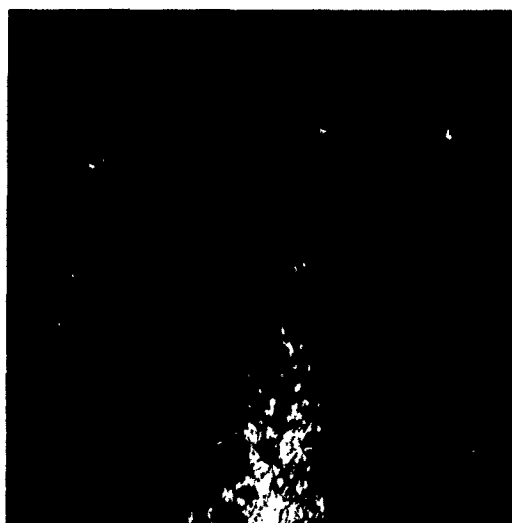
Figure 21d - F_n = 0.31

Figure 21 (Continued)
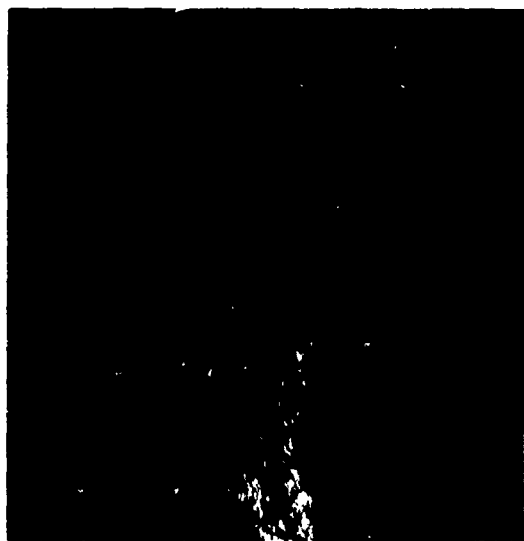
Figure 21e – F_n = 0.34

Figure 21f – F_n = 0.40
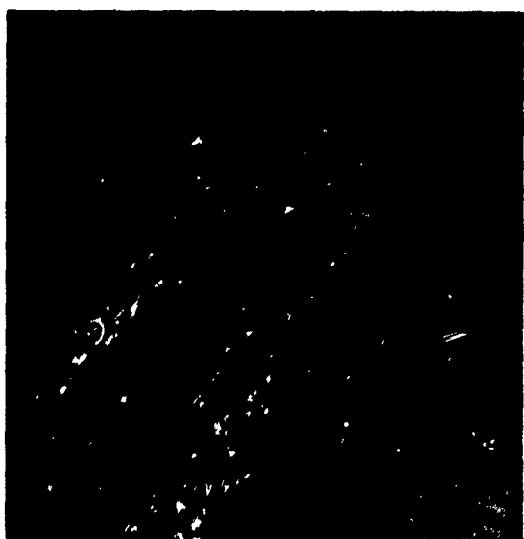
Figure 21g – F_n = 0.45

Figure 21h – F_n = 0.50

TABLE 1 - HULL FORM PARAMETERS FOR MODEL 5322

$\Delta/(0.01L)^3$	—	$52.370 (\text{tons/ft}^3)$
L/B	—	9.208
B/T	—	3.155
$\circledS$	—	7.628
ϕ	—	0.627
C_X	—	0.782
$\overline{FB}/L$	—	0.515
f_{BL}	—	0.0
f_T	—	0.055
B_T/B	—	0.642
T_A/T	—	0.089
i_E	—	6.4 deg
i_R	—	4.8 deg
i_B	—	6.0 deg

REFERENCES

1. Marwood, W. J. and A. Silverleaf, "Design Data for High Speed Displacement-Type Hulls and a Comp: cison with Hydrofoil Craft," Third Symposium on Naval Hydrodynamics, Scheveninger, Netherlands (1960).

2. Yeh, H. Y. H., "Series 64 Resistance Experiments on High Speed Displacement Forms," Marine Technology, Vol 2, No. 3 (Jul 1965).

3. Lindgren, H. and A. Williams, "Systematic Tests with Small, Fast Displacement Vessels, Including a Study of the Influence of Spray Strips," Society of Naval Architects and Marine Engineers Spring Meeting (1968).

4. Bailey, D., "New Design Data for High-Speed Displacement Craft," Ship and Boat International (Oct 1969).

5. St. Denis, M., "On the Transom Stern," Marine Engineering, Vol 58, pp. 58-59 (Jul 1953).

6. Saunders, H. E., "Hydrodynamics in Ship Design," 3 Vol, Society of Naval Architects and Marine Engineers, New York (1965).

7. Van Mater, P. R., Jr. et al., "Hydrodynamics of High Speed Ships," Stevens Institute of Technology, Davidson Laboratory Report 876 (Oct 1961).

8. Breslin, J. P. and K. Eng, "Resistance and Seakeeping Performance of New High Speed Destroyer Designs," Stevens Institute of Technology, Davidson Laboratory Report 1082 (Jun 1965).

9. Michelsen, F. C. et al., "Some Aspects of Hydrodynamic Design of High Speed Merchant Ships," Transactions of the Society of Naval Architects and Marine Engineers (1968).

10. Yim, G., "Analysis of Waves and the Wave Resistance to Transom Stern Ship," Journal of Ship Research, Vol 13, No. 2 (Jun 1969).

11. Yim, B., "Wavemaking Resistance of Ships with Transom Sterns, Eighth Symposium on Naval Hydrodynamics, Pasadena, California (Aug 1970).

12. Baba, E. and M. Miyazawa, "Study on the Transom Stern with Least Stern Waves," Mitsubishi Jyuko Giho, Vol 14, No. 1 (1977).

41

13. Vanden-Broeck, J. M., "Nonlinear Stern Waves," Journal of Fluid Mechanics, Vol 96, Part 3, pp. 603-611 (1980).

14. Haussling, H. J., "Two-Dimensional Linear and Nonlinear Stern Waves," Journal of Fluid Mechanics, Vol 97, Part 4, pp. 759-769 (1980).

15. Chang, M.-S. and P. C. Pien, "Hydrodynamic Forces on a Body Moving Beneath a Free Surface," First International Conference on Numerical Ship Hydrodynamics, Gaithersburg, Maryland (1975).

16. Dawson, C. W., "Practical Computer Method for Solving Ship-Wave Problems," Second International Conference on Numerical Ship Hydrodynamics, Berkely, California (1977).

17. Dawson, C. W., "Calculations with the XYZ Free Surface Program for Five Ship Models," Proceedings of the Workshop on Ship Wave Resistance Computations, Bethesda, Maryland (Nov 1979).

18. Chang, M.-S., "Wave Resistance Predictions Using a Singularity Method," Proceedings of the Workshop on Ship Wave Resistance Computations, Bethesda, Maryland (Nov 1979).

19. Troesh, A. et al., "Full Scale Wake and Boundary Layer Survey Instrumentation Feasibility Study," Department of Naval Architecture and Marine Engineering, College of Engineering Report, The University of Michigan (Jan 1978).

20. Sharma, S. D., "A Comparison of the Calculated and Measured Free-Wave Spectrum of an INUID in Steady Motion," Proceedings of the International Seminar on Theoretical Wave Resistance, University of Michigan, Ann Arbor, Michigan (Aug 1963).

21. Reed, A. M., "Documentation for a Series of Computer Programs for Analyzing Longitudinal Wave Cuts and Designing Bow Bulbs," DTNSRDC/SPD-0820-01 (Jun 1979).

INITIAL DISTRIBUTION

Copies		Copies	
1	WES	18	NAVSEA
			1 SEA 033
1	U.S. ARMY TRAS R&D		1 SEA 03D
	Marine Trans Div.		1 SEA 03R2
			1 SEA 05T
1	CHONR/100, A. Baciocco		1 SEA 05H
			1 SEA 312
1	CHONR/438, R. Cooper		1 SEA 32
			1 SEA 321
2	NRL		3 SEA 3213
	1 Code 2027		1 SEA 521
	1 Code 2629		1 SEA 524
			1 SEA 62P
1	ONR/BOSTON		1 SEA 6661 (D. Blount)
			3 SEA 996
1	ONR/CHICAGO		
		12	DTIC
1	ONR/NEW YORK		
		1	AFOSR/NAM
1	ONR/PASADENA		
		1	AFFOL/FYS, J. Olsen
1	ONR/SAN FRANCISCO		
		2	MARAD
1	NORDA		1 Div. of Ship R&D
			1 LIB
3	USNA		
	1 TECH LIB	1	NASA/HQ/LIB
	1 NAV. SYS. ENG. DEPT.		
	1 B. Johnson	1	NASA/Ames Res. Ctr, LIB
3	NAVPGSCOL	2	NASA/Langley Res. Ctr.
	1 LIB		1 LIB
	1 T. Sarpkaya		1 D. Bushnell
	1 J. Miller		
		3	NBS
1	NADC		1 LIB
			1 P. S. Klebanoff
1	NOSC/LIB		1 G. Kulin
1	NSWC, White Oak/LIB	1	NSF/Eng. LIB
1	NSWC, Dahlgren/LIB	1	DOT/LIB TAD-491.1
1	NUSC/LIB		

Copies			Copies		
2	MMA		3	Penn State	
	1	National Maritime Res. Ctr.		1	B. R. Parkin
	1	LIB		1	R. E. Henderson
				1	ARL LIB
4	U of Cal/Dept Naval Arch, Berkeley				
	1	LIB	1	Princeton U/Mellor	
	1	W. Webster			
	1	J. Paulling	1	U of Rhode Island	
	1	J. Wehausen		1	F. M. White
3	CIT		2	SIT	
	1	Aero LIB		1	LIB
	1	T. Y. Wu		1	Breslin
	1	A. J. Acosta			
			3	Stanford U	
1	Colorado State U/Eng Res. Ctr.			1	Eng LIB
				1	R. Street, Dept Civil Eng.
1	Cornell U/Shen			1	S. J. Kline, Dept Mech Eng.
2	Harvard U		1	U of VA/Aero Eng. Dept.	
	1	G. Carrier			
	1	Gordon McKay LIB	1	VPI	
				1	J. Schetz, Dept. Aero & Ocean Eng.
4	U of Iowa				
	1	LIB	3	Webb Inst.	
	1	L. Landweber		1	LIB
	1	J. Kennedy		1	Lewis
	1	V. C. Patel		1	Ward
4	MIT		1	SNAME/Tech LIB	
	1	LIB			
	1	J. R. Kerwin	1	Bell Aerospace	
	1	P. Leehey			
	1	J. N. Newman	2	Boeing Company/Seattle	
				1	Marine System
2	U of Minn/St. Anthony Falls			1	P. Rubbert
	1	LIB			
	1	R. Arndt	1	Bolt, Beranek & Newman/LIB	
3	U of Mich/NAME		1	Exxon, NY/Design Div. Tank Dept.	
	1	LIB			
	1	F. Ogilvie	1	Exxon Math & System, Inc.	
	1	Cough			
			1	General Dynamics, EB/Boatwright	

Copies		
1	Flow Research	
1	Gibbs & Cox/Tech Info	
1	Grumman Aerospace Corp./LIB	
5	Hydronautics	
	1 LIB	
	1 E. Miller	
	1 V. Johnson	
	1 C. C. Hsu	
	1 M. Tulin	
1	Lockheed, Sunnyvale/Waid	
2	McDonnell Douglas, Long Beach	
	1 T. Cebeci	
	1 J. Hess	
1	Northrop Corp./Aircraft Div.	
1	Science Application Inc./C. von Kerczek	
1	Sun Shipbldg/Chief Naval Arch.	
1	United Technology/East Hartford, Conn.	
1	Westinghouse Electric	
	1 M. S. Macovsky	

CENTER DISTRIBUTION

Copies	Code	Name
1	012	R. Allen
1	012.3	D. Jewell
1	1500	W. B. Morgan
1	1504	V. J. Monacella
1	152	W. C. Lin
2	1521	W. G. Day

Copies	Code	Name
2	1522	G. F. Dobay
5	1522	D. S. Jenkins
5	1522	T. J. Nagle
1	1522	T. Thomason
1	1522	M. B. Wilson
1	154	J. H. McCarthy
1	1542	B. Yim
1	1543	R. Cumming
1	1544	R. Brockett
1	1544	R. Boswell
1	1552	T. T. Huang
1	1552	H. T. Wang
1	1552	M.-S. Chang
1	1561	C. M. Lee
1	1564	J. Feldman
1	1568	G. Cox
5	1568	J. F. O'Dea
1	1606	T. C. Tai
1	1840	J. Schot
2	1843	J. Dean
1	1843	H. Haussling
1	1843	R. Vaneseltine
1	19	M. M. Sevik
1	194	J. T. Shen
1	1942	F. Archibald
1	1942	B. E. Bowers
10	5211.1	Reports Distribution
1	522.1	Unclassified Lib (C)
1	522.2	Unclassified Lib (A)

DTNSRDC ISSUES THREE TYPES OF REPORTS

1. DTNSRDC REPORTS, A FORMAL SERIES, CONTAIN INFORMATION OF PERMANENT TECH-
NICAL VALUE. THEY CARRY A CONSECUTIVE NUMERICAL IDENTIFICATION REGARDLESS OF
THEIR CLASSIFICATION OR THE ORIGINATING DEPARTMENT.

2. DEPARTMENTAL REPORTS, A SEMIFORMAL SERIES, CONTAIN INFORMATION OF A PRELIM-
INARY, TEMPORARY, OR PROPRIETARY NATURE OR OF LIMITED INTEREST OR SIGNIFICANCE.
THEY CARRY A DEPARTMENTAL ALPHANUMERICAL IDENTIFICATION.

3. TECHNICAL MEMORANDA, AN INFORMAL SERIES, CONTAIN TECHNICAL DOCUMENTATION
OF LIMITED USE AND INTEREST. THEY ARE PRIMARILY WORKING PAPERS INTENDED FOR IN-
TERNAL USE. THEY CARRY AN IDENTIFYING NUMBER WHICH INDICATES THEIR TYPE AND THE
NUMERICAL CODE OF THE ORIGINATING DEPARTMENT. ANY DISTRIBUTION OUTSIDE DTNSRDC
MUST BE APPROVED BY THE HEAD OF THE ORIGINATING DEPARTMENT ON A CASE-BY-CASE
BASIS.